A PULSE RADIOLYSIS STUDY OF THE FORMATION AND REACTIONS OF REDUCED METAL EDTA COMPLEXES

P. Buitenhuis

STELLINGEN

1. De verklaring die Kazuhiro Nhsawa *et al.* geven voor de lagere opbrengst van insertie in benzothiazol door recoil zwavel-atomen vergeleken met die van fotolytisch gegenereerde zwavel-atomen is onjuist.

   Kazuhiro Nhsawa and Ko Taki, Bull. Chem. Soc. Japan 50 (1977) 57

2. De pH-afhankelijkheid van het verval van het Cu(I)-complex met 5,7,7,12,14,14-hexamethyl-1,4,8,11-tetra-aza-cyclo-tetradeca-4,11 diene zoals gevonden door A.M. Tait *et al.* kan worden verklaard door meng-complexvorming met het product ontstaan uit de OH· en H· scavenger.

   A.M. Tait, M.Z. Hoffman and E. Hayon, Inorg. Chem. 15 (1976) 934

3. De bewering van A.N. Oblivantsev *et al.* dat na bestraling met deuteronen van $KMnO_4$ de retentie van het radioaktieve mangaan gelijk aan nul is, is niet geloofwaardig.

   A.N. Oblivantsev and N.F. Kulikov, Radiokhimiya 15 (1973) 136

4. Het hydronium ion-electron pseudoatoom als model voor het gehydrateerde electron stuit op praktische bezwaren.

   L.S. Levitt, Lett. a. Nuovo Cimento 15 (1976) 314

5. Ten onrechte verwaarlozen Neirinckx *et al.* bij de vergelijking van de aan de omgeving afgegeven energie ten gevolge van het verval van ^{125}I en ^{211}At de bijdrage van de conversie- en Auger-electronen in het geval van ^{125}I. De radiobiologische aspecten van hun experiment zijn derhalve onvoldoende uitgewerkt.

   R.D. Neirinckx, J.A. Myburgh, J.A. Smit in: Radiopharmaceuticals and labelled compounds, Vol. II, IAEA Vienna, STI/PUB/344 (1973) 171

6. Bij de afleiding van de formule voor de relatieve neutronen gevoeligheid van een grafiet-ionisatiekamer gevuld met CO_2, zoals gegeven in het ICRU-report 26, wordt het verschil in de verhouding van de kerma in weefsel t.o.v. die in CO_2 in het gamma-calibratieveld verwaarloosd. De hierdoor geïntroduceerde fout in de neutronendosis van een 15 MeV-bundel is onaanvaardbaar voor radiotherapeutische toepassingen, doch er kan gemakkelijk voor gecorrigeerd worden.

Neutron Dosimetry for Biology and Medicine, ICRU-report 26 (1977) 26

7. De door Heindel voorgestelde structuur voor het ^{131}I-chloroquine, gevormd door electrofiele joderíng van chloroquine, is zeer onwaarschijnlijk gezien de verdeling van de electronendichtheid in chloroquine.

   N.D. Heindel in: Nuclear Ophthalmology, ed.: M.N. Croll, L.W. Brady, P. Carmichael and R.J. Wallner, J. Wiley and Sons (1976) 104

8. Het verdient aanbeveling de efficiency van het "rookgenot" per sigaret op te voeren.

   Consumentengids (1975) 341 en (1976) 527

R. Buitenhuis
Amsterdam, september 1977

A PULSE RADIOLYSIS STUDY OF THE FORMATION AND REACTIONS OF REDUCED METAL EDTA COMPLEXES

ACADEMISCH PROEFSCHRIFT

ter verkrijging van de graad van doctor in de Wiskunde en Natuurwetenschappen aan de Universiteit van Amsterdam, op gezag van de Rector Magnificus, Dr. G. den Boef, hoogleraar in de Faculteit der Wiskunde en Natuurwetenschappen, in het openbaar te verdedigen in de Aula der Universiteit (tijdelijk in de Lutherse Kerk, ingang Singel 411, hoek Spui) op woensdag 14 september 1977 te 13.30 uur.

door

ROBERT BUITENHUIS

geboren te Apeldoorn

1977

Promotor : Professor Dr. A.H.W. Aten Jr.
Co-referent: Dr. L. Lindner

The work described in this thesis is part of the research program of the Institute for Nuclear Physics Research (IKO), made possible by financial support from the Foundation for Fundamental Research on Matter (FOM) and the Netherlands Organization for the Advancement of Pure Research (ZWO).

Aan mijn ouders

Aan Rinske, Remko en Rosemarije

Cover: paraglyphic impressions of the optical part of the pulse radiolysis system in front of the drift tube of the linear accelerator.

CONTENTS

CHAPTER I

INTRODUCTION

1.1 The pulse radiolysis technique

Until 1960 the fundamental processes underlying the interaction of ionizing radiation with a chemical system were investigated mainly by indirect methods: the products resulting from the interaction were analyzed after irradiation and the chemical mechanism was inferred from these data. By changing the reagents and their concentrations one was able to obtain an insight in the primary processes. The drawback of such procedures is that the number of parameters is so large that often an explanation of the experimental results is uncertain if not impossible.

About 1960 it became possible to investigate these processes more directly. Accelerators, which were able to deliver very short pulses of ionizing radiation became available, e.g. linear microwave accelerators, Van de Graaff accelerators and, more recently, Febetrons. These accelerators made it possible to develop the pulse radiolysis technique, which is similar to the flash photolysis technique [1]. In the case of pulse radiolysis the transient species are generated by means of a very short pulse of ionizing radiation, and they are usually measured by means of a spectrophotometer set-up or a spectrograph [2]. The difference between pulse radiolysis and flash photolysis from a chemical point of view is that the energy of the particles which cause the perturbation, is of the order of the energy of the chemical bond in the latter case and of the order of MeV's in the former case. This means that while in photolysis it is possible to activate exclusively the selected processes, in radiolysis

the energy deposition is not specific for one kind of electronic transition [3], i.e. the energy will be deposited predominantly on the solvent molecules because of their high concentration.

The concentration of the species involved are determined by measuring their (specific) light absorption as a function of time after the pulse of ionizing radiation. This method is only applicable when the absorption coefficients are known and sufficiently high. A detailed description of the system used by us is given in Chapter II. One of the aims of this work was to obtain the technical know-how of the pulse radiolysis technique with the linear electron accelerator (EVA) of the Institute for Nuclear Physics Research in preparation of pulse radiolysis research with the new linear accelerator under construction (MEA).

The characteristics of the microwave electron accelerator used were most suitable for studies on the microsecond time scale, which often can be performed in aqueous solutions. The principal aim of this study was to obtain a better understanding of the role of metal ions in the radiation chemistry of aqueous systems. This investigation also has a bearing on other work in progress regarding radiation chemical effects in solid matrices containing water of crystallization.

1.2 The radiolysis of water

To study the radiolysis of aqueous solutions it is important to understand the radiolysis of water because the energy of the ionizing radiation is deposited predominantly on the solvent molecules due to their concentration. The initial energy deposition is not homogeneous but occurs in spurs [4]. Spurs are small regions in which a few pairs of radicals and ions are formed. In the case of electrons with energies in the MeV-range these spurs are isolated. These radicals diffuse outwards until a homogeneous distribution is reached. In the case of water H_2, H_2O_2 and H_2O are formed from the radiation induced H· and OH· radicals during this

inhomogeneous stage. Calculations describing this process have been performed by Kuppermann [5]. These calculations show that after approximately 10^{-8} s the homogeneous stage is reached. The yields of the radiolytic products at that time are called the "primary yields" and are denoted by the respective "G-values" (e.g. G_{H_2}): the number of product molecules obtained per 100 eV deposited.

Mozumder and Magee [6] distinguish between three entities: spurs, with a maximum energy content of 100 eV, blobs (100 - 500 eV) and short tracks (0.5 - 5 keV). The latter two are caused by secondary electrons generated by knock-on processes. In the case of blobs the secondary electron has not enough energy to go far from its origin, in the case of short tracks the energy of the secondary electron is not sufficient to create isolated spurs. Due to their higher local ionization density short tracks and blobs create a higher relative yield of H_2 and H_2O_2 than spurs do.

The interaction of accelerated electrons with the water molecules involves excitation and ionization followed by chemical reactions:

$$H_2O \rightsquigarrow H_2O^* \qquad (1)$$

$$H_2O \rightsquigarrow H_2O^+ + e^- \qquad (2)$$

$$H_2O^* \rightsquigarrow H\cdot + OH\cdot \qquad (3)$$

$$H_2O^+ + H_2O \rightarrow OH\cdot + H_3O^+ \qquad (4)$$

During the radiolysis of water, the hydrated electron (e^-_{aq}) is formed. This is an entity consisting of an electron stabilized by its own hydration shell. Magee postulated [7] that the electron produced by reaction (2) returns rapidly to its parent ion yielding excited molecules which dissociate into H·, OH· and e^-_{aq}. Platzmann [7] assumed that the electron escapes from its parent ion and becomes hydrated. These two theories suggest a different distribution of the radicals formed in the spur.

In the expanding spur the radiation induced products react with each other, e.g.:

$$H\cdot + H\cdot \rightarrow H_2 \quad (5)$$

$$OH\cdot + OH\cdot \rightarrow H_2O_2 \quad (6)$$

$$H\cdot + OH\cdot \rightarrow H_2O \quad (7)$$

$$e^-_{aq} + H_3O^+ \rightarrow H\cdot \quad (8)$$

$$e^-_{aq} + OH\cdot \rightarrow OH^- \quad (9)$$

$$e^-_{aq} + H\cdot \rightarrow H_2 + OH^- \quad (10)$$

After the homogeneous stage is reached (10^{-8} s) these reactions can be summarized by:

$$H_2O \rightsquigarrow e^-_{aq},\ H_3O^+,\ OH^-,\ OH\cdot,\ H_2O_2,\ H_2 \text{ and } H\cdot \quad (11)$$

After $\sim 10^{-8}$ s these products react further with each other and with the solutes in the system, as long as the concentrations and the reactivities of these solutes are not so large that they react already in the spurs.

1.3 The reaction of the hydrated electron with metal complexes

The solvated electron is a very powerful reducing agent ($E^0 = 2.77$ V [8]). It is also the most simple reducing agent known: it disappears during reaction. In addition it has an intense absorption spectrum (cf. Chapter II), which makes it possible to follow its reaction by the optical pulse radiolysis technique. Consequently the solvated electron enables one to investigate the redox-properties of a whole series of substrates such as metal complexes. The study of metal complexes has also a bearing on the radiolysis of biological systems [9-12]. The factors one would like to investigate are the influence of the metal (type, redox potential), the ligand (H_2O or e.g. EDTA = ethylene diammine tetra acetic acid) and the chemical properties of reduced complexes, generated by the hydrated electron.

The influence of the type of metal and ligand on the rate of reaction with e^-_{aq} was studied on numerous occasions [13]. Anbar *et al.* [14,15] tried to explain the

differences between the values of the rate constants of the reactions of solvated electrons with metals complexed either with water or with EDTA by means of the Marcus theory [16].

This theory relates the rate constant of redox reactions to the free energy effect (ΔF^{o}) of the reaction and the energy (λ) necessary to rearrange the reactants and the solvent molecules to a configuration in which electron transfer is possible according to the Franck-Condon restriction. However, EDTA complexes react in general one or two orders of magnitude more slowly than the corresponding hydrated metal ions do. This leads to the conclusion that the difference in the corresponding ΔF^{o} and thus the redox potential of the M(II)/M(I) couple involved has to be unrealistically large. Neither can the difference in reactivity be explained by a difference in λ [15].

A really satisfactory theoretical model describing these reactions of the hydrated electron would require a thorough knowledge of the chemical and physical properties of the reduced product.

1.4 Some aspects of reaction kinetics

The rates of the chemical reactions occurring as a consequence of the interaction of ionizing radiation with solutions are determined by measuring as a function of time, the concentrations of one or more of the species involved. In our case this is accomplished by observing the absorption spectrum. The rates are often very high, sometimes limited only by the rate at which the reactants diffuse in the solvent, so-called diffusion-controlled reactions. According to Smoluchowski [17] and Debye [18] one can derive for the rate constant of such reactions:

$$k_{diff} = \frac{4\pi r_{ab} D_{ab} N}{1000} \left\{ \frac{Z_a Z_b e^2}{r_{ab} \varepsilon kT} \Big/ \left[\exp\left(\frac{Z_a Z_b e^2}{r_{ab} \varepsilon kT} \right) - 1 \right] \right\} \; M^{-1} s^{-1}$$

r_{ab} = sum of radii of the reactants
D_{ab} = sum of the diffusion coefficients

N = Avogadros number

Z = charge

e = charge of the electron

ε = dielectric constant

k = Boltzmann's constant

T = temperature.

The order of magnitude of k_{diff} is $\geq 10^{10}$ $M^{-1}s^{-1}$ for the species commonly encountered in radiolysis of water.

The rate of reaction is affected by the ionic environment of the reactants in the solution, the so-called primary salt effect. Defining the ionic strength as $\mu = \frac{1}{2} \Sigma m_i z_i^2$ (m_i = molality, z_i = charge of the i^{th} ionic species present in the system) one can derive according to Brønsted, Bjerrum, Debye and Huckel [19]

$$\log \left(\frac{k_{obs}}{k_o}\right) = \frac{1.02\ Z_a Z_b \sqrt{\mu}}{1+0.329\ r_{ab}\sqrt{\mu}}$$

k_{obs} = observed rate constant

k_o = rate constant at infinite dilution of ions.

These two equations make it possible to calculate the reaction rate, if the reaction is diffusion controlled. Comparison of this value with the experimental one will reveal whether the reaction is essentially diffusion controlled or not. In the latter case it may be possible to evaluate the mechanism of the reaction, by comparing rate constants of a series compounds in which one parameter is changed.

Since there are more than one primary species, there are also more than one reactions occurring simultaneously during radiolysis. However, it is often possible to convert interfering species into less interfering ones by the addition of scavengers. These are reagents, which react fast and more or less specifically with one of the primary species. By changing the chemical parameters of the system, e.g. concentrations of the reagents, pH, ionic strength and so on, it is possible to obtain information concerning the reaction scheme.

References

1) G. Porter, Proc. Roy. Soc. A, 200 (1949) 284
2) L.M. Dorfmann and M.S. Matheson in: Progress in Reaction Kinetics, Vol. 3, Ed. G. Porter, Pergamon Press, Oxford (1965) 244
3) A. Mozumder in: Advances in Radiation Chemistry, Vol. 1, Wiley-Interscience, New York (1969) 22
4) J.K. Thomas, *ibid.*, 119
5) A. Kuppermann in: Radiation Research, Ed. G. Silini, North Holland Publ. Company, Amsterdam (1967) 212
6) A. Mozumder in: Advances in Radiation Chemistry, Vol. 1, Wiley-Interscience, New York (1969) 63
7) J.K. Thomas, *ibid.*, 110
8) E.J. Hart and M. Anbar, The Hydrated Electron, Wiley-Interscience, New York (1970) 62
9) G. Wilting, Ph.D. Thesis, Rijksuniversiteit Utrecht (1974)
10) M. Faraggi in: Fast Processes in Radiation Chemistry and Biology, Ed. G.E. Adams, E.M. Fielden, B.D. Michael, Wiley (1975) 285
11) I. Pecht and M. Goldberg, *ibid.*, 277
12) E.M. Fielden, P.R. Roberts, R.C. Bray, D.J. Lowe, G.N. Mautner, G. Rotilio and L. Calabrese, Biochem. J. 139 (1974) 49
13) M. Anbar, M. Bambenek and A.B. Ross, NSRDS-NBS 43 (1973)
14) E.J. Hart and M. Anbar, The Hydrated Electron, Wiley-Interscience, New York (1970) 117, 179
15) M. Anbar and D. Meyerstein, Trans. Far. Soc. 65 (1969) 1812
16) R.A. Marcus, J. Chem. Phys. 43 (1965) 3477
17) M. Smoluchowski, Z. Phys. Chem. 92A (1918) 129
18) P. Debye, Trans. Electrochem. Soc. 82 (1942) 265
19) C. Capellos and B.H.J. Bielski, Kinetic Systems, Wiley-Interscience, New York (1972) 119

CHAPTER II

EXPERIMENTAL SET-UP, PERFORMANCE

2.1 *Introduction*

Early pulse-radiolysis experiments mostly operated as a single shot sequence, in which the transient is recorded by means of an oscilloscope and a polaroid camera [1,2]. Several devices exist to convert the photographic image into a digital form. e.g. ref. [3]. In later experiments the transient signal was converted into a digital form by means of a transient-recorder, e.g. ref. [4].

Several years ago it was decided in this laboratory to develop a pulse-radiolysis set-up, that takes advantage of the high repetition rate of the linear electron accelerator of the Institute, and to avoid the use of photographic recording of the transient absorptions.

The accelerator is an s-band electron accelerator with a maximum energy of 85 MeV [5]. The high energy obtainable makes it possible to use quite long irradiation cells with the electron beam directed along the axis. The dose-distribution in the 1 cm cuvettes as used in all the experiments described, is very uniform [6]. For pulse-radiolysis experiments the accelerator is operated under the following conditions: e^--energy of about 40 MeV, repetition rate of 25 pulses per second, pulse length of 0.5 - 1 μsec, peak current of 10 - 30 mA. The aluminium exit window for the electrons is approximately 0.2 mm thick. The position of the electronbeam can be checked adequately on a closed circuit T.V. by visualisation on a BeO screen.

2.2 *Optical system*

The lay-out of the optical system is shown in fig. 1.

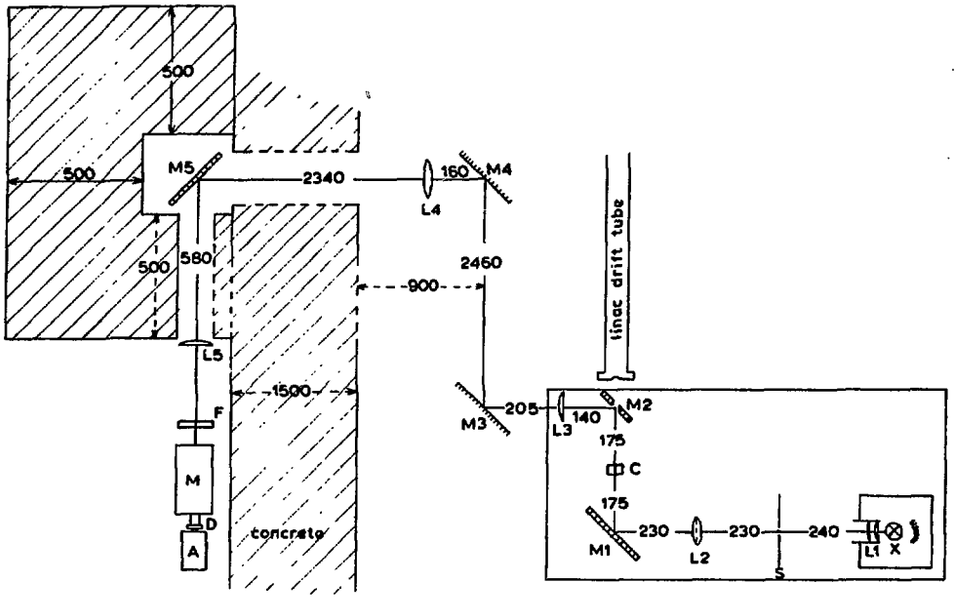

Fig. 1 Lay-out of the pulse-radiolysis system. All dimensions are in mm. X is the Xenon-lamp, S a slit system, L_1, L_2,....., L_5 are Suprasil lenses, M_1, M_2, ..., M_5 are first surface reflectors, C is the irradiation cell, F the absorption filter, M the monochromator, D the detector, A the amplifier.

It is of a conventional design. However, while usually the monochromator provides the limiting aperture, in this case a 100 mm absorption cell, with an internal diameter of 19 mm was chosen to define the limiting aperture. Furthermore, the direction of the electron and light beams are not transverse as usual, but under 180°, thus reducing the possible interference due to the Cerenkov emission to a minimum only detectable at short wavelengths.

In the following section the different parts will be

discussed briefly.

The light source consists of an OSRAM XBO 450 Xenon lamp (X in Fig. 1) fed by a VARIAN P - 500S - 1 power supply.

The light output of the lamp was kept constant within 1% by regulating the lamp current. The light intensity is monitored by means of a BPX 25 photodiode inside the lamp-housing. This photodiode controls a feed back circuit in the power supply (Fig. 2).

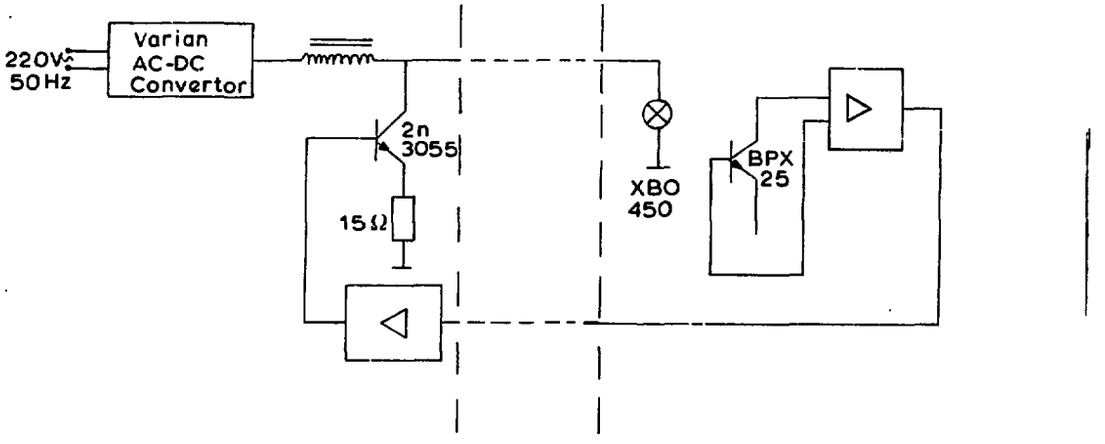

Fig. 2 Diagram of the light stabilization circuit of the Xenon lamp

This circuit suppresses completely a 600 Hz modulation which is generated by the VARIAN power supply. The only light modulation left is a 100 Hz ripple with an amplitude of 1%. Because this is slow in comparison with the duration of the measurement, and because the measurements and the ripple are synchronous, this modulation was considered acceptable.

The original ORIEL OPTICS C60-53 lamphousing had to be replaced by a sturdier construction to reduce intolerable lamp vibrations resulting from the cooling fan and to improve the mechanical stability.

The lamp housing is equipped with a f = 50 mm, f/1.0

quartz condensor (L1 in Fig. 1), which depicts the lamp arc on a horizontal and vertical adjustable slit system S. The slit is depicted in the irradiation cell C by means of a biconvex Suprasil lens L2 (Hereaus, f = 150 mm, diameter 80 mm). This image is depicted on a biconvex Suprasil field lens L4 (Bleeker, f = 1440 mm, diameter 108 mm) by planconvex Suprasil lens L3 (Hereaus, f = 300 mm, diameter 90 mm). Next comes a planconvex Suprasil lens L5 (Bleeker, f = 440 mm, diameter 98 mm), which gives an image of the slit system S on the entrance slit of the monochromator M: Bausch & Lomb, high intensity monochromator: housings 33 - 86 - 25 and 33 - 86 - 26, gratings 33 - 86 - 02 (350 - 800 nm), 33 - 86 - 07 (200 - 700 nm) and 33 - 86 - 03 (0.7 - 1.6 μm). The monochromator assemblies are carefully calibrated with discharge lamps (Ultraviolet Products, Philips) over the whole range. Second order reflections and stray light are suppressed by absorption filters in front of the monochromator (Schott & Gen., types GG and RG).

All optical parts are mounted in commercially available optical bench components (Spindler and Hoyer). Because the accelerator is also used for other purposes, the major part of the system is mounted on a cart, that can be positioned with a reproducibility of less than 0.3 mm by means of rails and pawls. This makes it possible to remove all sensitive equipment from the accelerator bunker.

As has been mentioned already, the analyzing light beam passes the cell parallel to the electron beam. In order to prevent the destruction of mirror M2 by the electron beam, this mirror has a 6 mm hole in the centre. All mirrors (M1, M2,....., M5) are first-surface reflectors (Spindler and Hoyer).

The maximum cell length that can be used is 100 mm, but the actual measurements were performed with 10 mm cells. Cells are mounted in a water cooled copper sample changer with 5 positions.

The small bunker around mirror M5 acts as a very

effective labyrinth against leakage of secondary neutrons, even when the accelerator is used at a high power level for other experiments.

2.3 Detection system

As a light detector a PIN-10 UV enhanced Schottky Barrier Silicon photodiode (United Detector Technology) with an active area of 1.25 cm^2 was chosen. According to the specifications, the output of this detector is linear up to a photocurrent of 10^{-3} A. This type of detector has a maximum quantum efficiency of approximately 70% and is sensitive between 300 and 1050 nm. The dark current is of the order of 10^{-7} A at a bias of 50 V. (Specification of the manufacturer: 5×10^{-7} A at a bias of 10 V.) The rise time of the detector (50 V bias, 50 Ω) is quoted as 10 nsec, but it is known [7] that such a figure has to be redetermined.

Under the conditions of our experiment, in which the detector current is fed directly into a modified charge amplifier, the total charge collection time is < 40 nsec for the UV enhanced detector. (For the standard detector, not UV enhanced, this time is somewhat shorter.)

For the experiments to be described these numbers are of secondary importance, because ultimately samples with a width of 800 nsec are taken from the signal. This means that any signal faster than 800 nsec will be integrated in the (sampling) electronics used for the digital conversion described in the next section.

Figure 3 schematically represents the first amplifier (A in Fig. 1). Figure 4 shows the characteristics of this amplifier. It is evident that in the interval between 1 msec and 10 msec the amplification varies with time. This feature is taken into account in the computer programs used to analyze the data. During the first msec the A.C. component of the transient signal is amplified by a factor of 10 with regard to the D.C. component, without separating the two. This makes

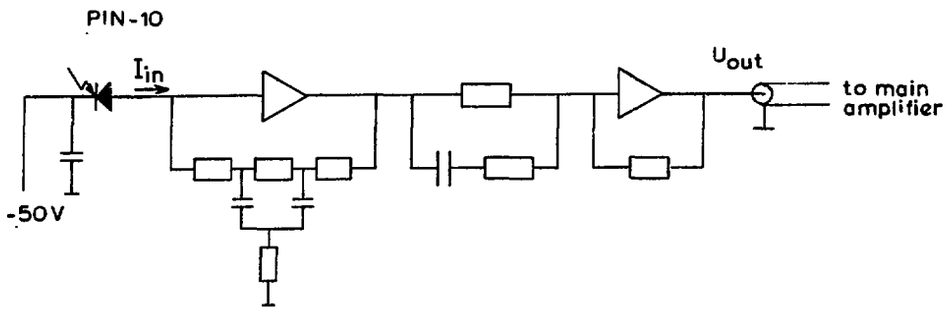

Fig. 3 Diagram of the charge amplifier

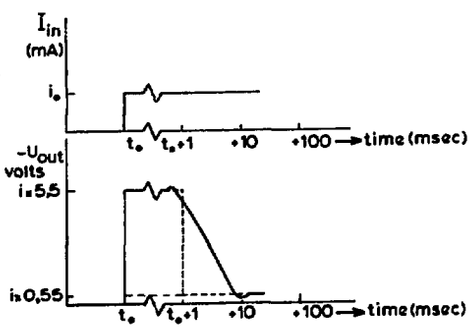

Fig. 4 Characteristics of the charge amplifier. The input I_{in} is given in mA, the negative output U_{out} in volts. The dashed line represents the idealized characteristics, the solid line the actual characteristics for which the computerprogram corrects the experimental points.

it possible to determine weak absorptions with greater precision, together with the unperturbated light before or after the pulse, but on the other hand it limits the maximum absorption to 10%.

The signal from this amplifier is fed into a main amplifier, which gives it the right amplitude for the analyzer.

2.4 Registration of the transient signal

2.4.1 Hardware

The main part of the equipment used for the digitalization and registration of the transient signal is a multichannel analyzer array used for nuclear spectroscopy. It consists of a 4096 channel ADC (Laben FC60/4096) interfaced with a PDP8/I computer equipped with an extended memory (8k), a 32k word magnetic disc, a storage scope (Tectronics, type 611 equipped with a KV8/I controller), a 75 ips 800 bpi 7 track tape unit (Pertec 6840-75-75) and a fast paper tape reader and puncher.

In order to use this equipment for pulse-radiolysis experiments several considerations had to be taken into account. First, the timing had to be matched with the accelerator. Second, the ADC is only capable of digitalizing pulses, because it is used for nuclear spectroscopy purposes. Third, the ADC needs approximately 25 μsec to digitalize one pulse. One should also keep in mind that because of the 25 Hz repetition rate of the electron accelerator consecutive electron bursts lie 40 msec apart, which means that ample time is available to observe the transient and to handle the accumulated data in the PDP8/I. The block-diagram of the system is shown in Figure 5.

The registration of a transient occurs as follows: the modulator of the accelerator gives an attention pulse (about 4 μsec prior to the electron burst of about 1 μsec). This causes the Schmitt-trigger to set the S.R.-flipflop, which opens a gate. The pulses from the 1 MHz clock are fed into a 8-bit scaler (÷64), which gives an overflow every 64 μsec. This overflow opens a linear gate (during a 800 nsec time interval) which supplies the ADC with an analog pulse. If the PDP8/I delivers a stop-level this overflow also causes the flipflop to reset. As long as the PDP8/I delivers a start-level no reset takes place, and the linear gate will be opened every 64 μsec. By delivering a start-level prior to the attention pulse, and a stop-level after the information

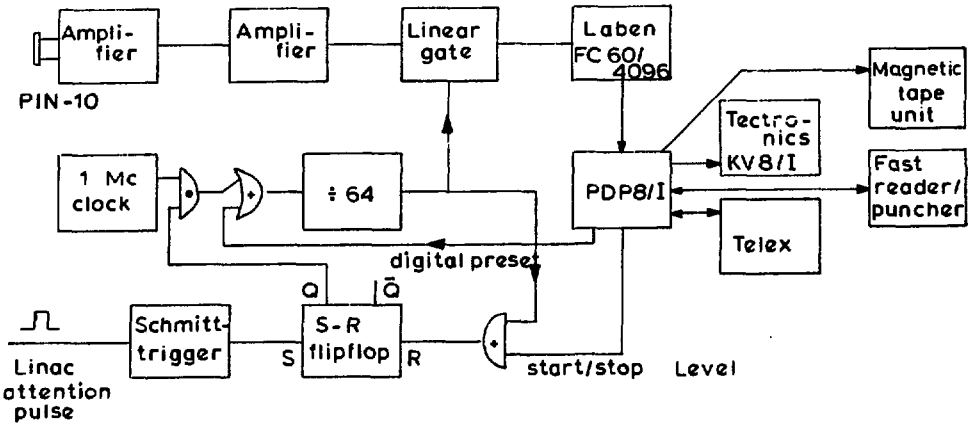

Fig. 5 Block-diagram of the data acquisition and storage array

needed from one transient is accumulated (but before the next attention pulse has arrived) it is possible to measure one transient with samples 64 μsec apart. A digital preset of the 8-bit scaler before the attention pulse shifts the time base by a corresponding number of μsec. By choosing the right sequence of presets it is possible to measure at will with apparent sampling intervals of 1, 2, 4, 8, 16, 32 or 64 μsec. The use of a 1 MHz clock for this time base introduces a time uncertainty of 0.5 μsec.

In order to test the performance of the system as a whole, an electronic device was constructed, which supplies an attention pulse similar to the one supplied by the linac, as well as a well-defined modulated light signal similar to a transient absorption.

2.4.2 Data compilation

Figure 6 shows a typical example of a histogram of a transient absorption due to solvated electrons in water recorded on a punched paper tape and drawn by means of a Cal-

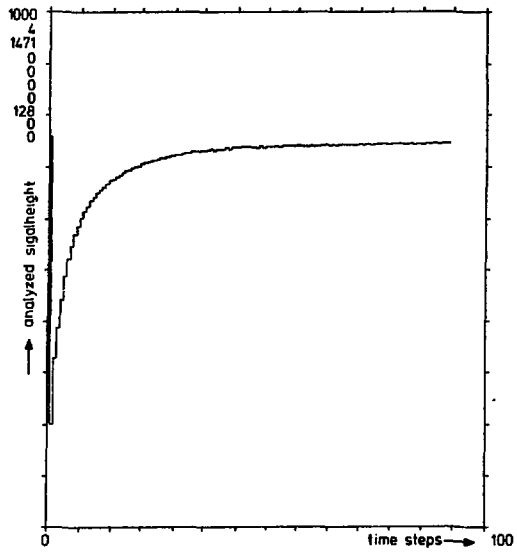

Fig. 6 Typical example of a histogram of a transient absorption due to solvated electrons in water, p_H = 12, 0.5 percent n-butanol added. The curve is constructed out of 1008 electron bursts. Each time-step represents 4 μsec, and is an average of 63 measurements

com-plotter. The curve is constructed from a total of 1008 transients, obtained with a repetition rate of 25 pulses per second. The absorption was measured every 64 μsec (overflow 8-bits register) during a 800 nsec time interval. In order to obtain apparent sampling intervals of 4 μsec, the time-base of each sequence of data generated by one burst of the linac was shifted with respect to the previous one by 4 μsec (by presetting the 8-bits register by the PDP8/I). Thus 16 subsequent electron bursts give rise to one complete transient curve. As a total of 1008 bursts was administered, each point

on the histogram is the average of 63 measurements.

In addition, 19 msec after each attention pulse another point can be sampled. This reading is supposed to represent the zero-absorption, of which the value averaged over all transients, is listed among the numbers to the left of the vertical axis in Fig. 6 (in this case 1471). Because the timing of the electron gun can be shifted with respect to the modulator pulse (4 μsec long) it is possible to start the analyzing sequence a few μsec before the electron burst. Also in this way a measurement of the zero-absorption level can be obtained.

The dark current and accelerator-generated (synchronized) noise can be measured by running the experiment at a wavelength below the sensitive wavelength of the detector or by intercepting the light before the monochromator.

2.4.3 Software

A flowsheet of the PDP-computer program is given in Figure 7. The program begins to ask for both the number of transients that have to be sampled and the desired apparent time interval between the samples. The program clears a 128 word buffer and a memory file, the last one is used for storing the sum of the data from the buffer and the data from the previous transients. The very first linac attention pulse results only in an interrupt from the ADC, which indicates that the accelerator has been started. This causes the PDP8 to preset the 8-bits scaler according to the desired apparent sampling intervals and to generate a start level. The second attention pulse initiates the analysis of the first transient as described above, which results in 128 data points which are stored in the buffer. After that the synchronization counter, which keeps track of the timing sequence, is up-dated. Then there is a period of adding the buffered data to the data in the memory file. The ADC is read out once more 19 msec after each attention pulse, and this value can be taken as the zero-absorption level of that

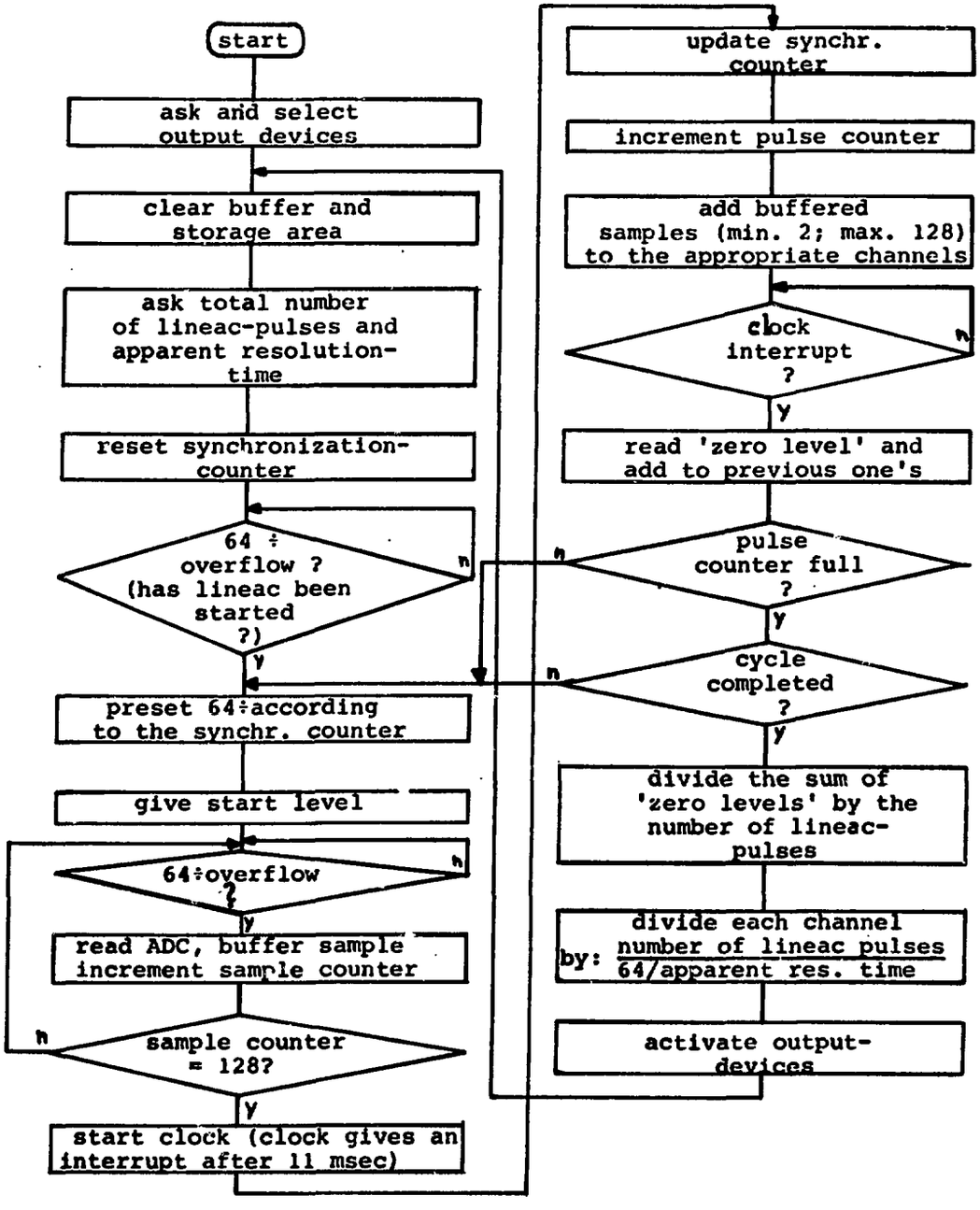

Fig. 7 Flow-sheet of the pulse-radiolysis computer program

particular transient. This number is added to the sum of previous zero-absorption values. Subsequently the start/stop level is set at "stop", and the sequence is repeated: preset the 8-bits scaler, generate a start level, wait for the next attention pulse and so on. After the required number of measurements is reached, the results can be typed, punched, or outputted on magnetic tape and displayed on a storage scope.

2.5 Processing of the data

2.5.1 Data conversion

The PDP8/I delivers the raw data on magnetic tape or punched papertape in the form of 128 uncorrected light intensities and an administrative record. For the conversion of these data a program named PULK was written. PULK is coded in FORTRAN and can be run either on the PDP-10 computer of our Institute, or on a CDC-Cyber computer, located elsewhere. The program operates as follows:

First there are interactive questions with regard to the selection of any set of particular experiments out of a file and with regard to instructions where to store the results. Then the experimental data are processed in order. From the bookkeeping record, the light intensity at a time 19 msec after the attention pulse is read; either this figure or one computed from the intensities in the first µsec or one computed from the last ten measured channels is chosen as the zero-light level.

In the next procedure the data are corrected for the effects introduced by the pre-amplifier (the 10-fold enhancement of the A.C. component during the first msec and the changing amplification during the following 9 msec) and by the main amplifier (a thermal drift effect introduced by differential amplification). In the case of the pre-amplifier this is achieved by solving a set of differential equations, which represent the inverse effect of the filters used in the pre-amplifier. After these corrections have been applied, the true values for the light intensities are available.

Subsequently absorptions and optical densities are calculated and printed on the line printer. The logarithm of the optical density is also represented graphically on the line printer to provide a preliminary evaluation of the experiments. The optical densities are also filed on the disk of the PDP-10 for further calculations. Because the data are stored in the same format as gamma-ray spectra measured in this Institute, operations available for application to these spectra, could also be carried out with our particular data, e.g. plotting on a CALCOM-plotter (Fig. 6) and copying on other storage media.

2.5.2 *Data reduction and model computations*

In the present configuration it is possible to irradiate about 25 different samples during an experimental run lasting several hours. Therefore, a large amount of measurements has to be analyzed afterwards. To facilitate this the program KLPP was written. This program runs on the PDP-10 and is fully interactive. The input is formed by the files on the disk delivered by the program PULK. The output is a list on the line printer containing all values of the administrative record as there are:

Number of the experiment and sample, apparent time intervals between the samples of the detector signal, wave length and slit width of the monochromator, peak current, duration and number of linac pulses and the zero-light intensity after 19 msec. Furthermore, the list contains the following computed items:

i) the first-order decay constant and apparent half-life together with the time limits of the calculation (as asked by the program before), and
ii) an extrapolation of the optical density to the time immediately after the electron pulse.

These items are computed by fitting a straight line through the logarithm of the optical density by means of a simple least squares method.

The experimental data can be divided into two classes: one in which the decay is (pseudo-) first-order and one in which this is not the case. In the first class the KLPP program suffices for data analysis. In the second class this is, of course, not true. However, by taking the experimental data over a short time interval immediately after the electron pulse, one can obtain a better approximation of the optical density immediately after the pulse than one obtains by taking only the value of the first data point after the electron pulse.

The data from the experiments in which no first-order kinetics were observed, are not analyzed by means of a straightforward procedure, but instead the program WR16 from Argonne National Laboratory is used [8]. This program was converted from the published form intended for a CDC-3600 computer to forms suitable for the DEC PDP-10 or the CDC-Cyber computer. The program calculates, as a function of time, the concentrations of species taking part in the simultaneous first- and second-order chemical reactions induced by ionizing radiation. Also the optical absorbance is calculated. As input the program requires all chemical reaction equations with rate constants, a list of all relevant species with G-values, initial concentrations, and extinction coefficients together with the dose rate as a function of time.

In our version the results are printed and - in a condensed form - filed on the disk of the PDP-10. By varying only one rate constant at a time sets of data are created on the disk that can be plotted together with the experimental data by the program PLOTWR to evaluate a particular rate constant. As input PLOTWR uses data from disk or teletype (interactively or batch) and it contains the routines delivered by GENPLT II [9], a general plotting package.

2.6 Limitations of the system

There are several limitations to the system as it is used. One has already been mentioned: the absorption must not

exceed 10%.

A second one is that the synchronization between accelerator and detection system is gouverned by a 1 MHz clock, which introduces a time uncertainty of 0.5 μs. This clock can not be speeded up, since in that case the pre-setting of the timer by means of the PDP8/I becomes impossible because of the interfacing.

Also, in the case of high doses, it is necessary to renew the sample (either discontinuously or continuously), to eliminate the interferance of radiation induced impurities.

In the time interval between 1 msec and 10 msec the amplification of the pre-amplifier decreases by a factor 10. This is corrected for in the PULK program, but it affects, of course, the quality of the measurements in this time range. On the other, in this region one will measure with an apparent (and also true) sample interval time of 64 μs, making a more effective use of the information gained from one electron burst (for shorter - apparent - interval times a larger number of electron bursts is needed for one measuring cycle).

2.7 Preparation of the chemical samples

2.7.1 Quality of the chemicals

All chemicals used were purchased from "Merck". If the "Suprapur" quality was not available, "AR"-grade chemicals were used. These were recrystallized from ultra pure water in the case of $PbCl_2$, EDTA, KCNS and most of the sulphates. The water content of the recrystallized salts was determined by the Karl Fischer method.

The water used for the recrystallization was purified in the system quoted in the next section.

The alcohols were either used as received or purified by destillation using a spinning band column (Perkin-Elmer 251 Auto Annular Still). The purity was checked by gaschromatography.

All glassware was cleaned by standing overnight in a bichromate-sulphuric acid solution. Prior to use it was rinsed four times with purified water and steamed. All solutions were prepared in standard volumetric glassware.

2.7.2 Water purification system

For the initial experiments water was purified by distillation. The starting material was demineralized water (typical conductivity less than 0.5 µS) produced in our laboratory. This water was distilled in four steps: over $KMnO_4/NaOH$, over $K_2Cr_2O_7/H_2SO_4$ and twice without an additive in an all quartz apparatus. The whole system was guarded by level controls and protected against overheating and running dry.

As it turned out in the experiments the quality was not stable with respect to organic impurities, probably due to organic pollution of the tapwater in Amsterdam. To solve this problem, which was getting steadily worse, several different arrangements in front of the distillation system were tried, one of which was direct pre-distillation of tapwater followed by a treatment with ozone. Neither method was really satisfactory, because every time a deposit of organic material was formed before the last distillation step.

The problem was solved by replacing the distillation system by a Millipore "Milli Q2"-system, consisting of four columns: a pre-filter 0.04 µm (CP 04 010 03), an activated charcoal filter (CDAC 012 04), two ion-exchange elements (CDMB 012 04), all part of a circulatory system and a final filter 0.022 µm (PMEG 090 02). The system was fed with demineralized water from the laboratory system. In this way a satisfactory quality was obtained, which can be compared with the best water prepared with the distillation system described. A special advantage of this system is the high throughput in comparison with the cumbersome distillation procedure.

The quality of the water was tested with Fricke dosimeter solutions with and without NaCl added and irradiated

with the gamma-radiation of a ^{60}Co source. From the difference in the G-values measured a judgement about the purity with respect to organic materials can be made.

2.7.3 Deoxygenation of the samples

Because oxygen has a high reaction rate with most "transients" deoxygenation of the samples is extremely important. The Suprasil cuvettes (Hellma 221QS, 1 cm optical pathlength) were equipped with a sphere (cf. Fig. 8), to make it possible to deaerate the samples by means of the freeze-thawing technique. This procedure was repeated three times, after which the cell was sealed.

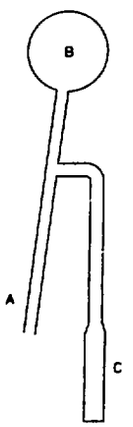

Fig. 8 Construction of the vacuum cuvette. A: point to be melted; B: sphere for the freeze-thawing cycles; C: fused quartz cuvette.

The vacuumline used consisted of a simple greaseless manifold and was evacuated by a three-step method consisting of a "Speedivac" rotationpump (Edwards) equipped with a liquid nitrogen baffle, a sorption pump and an ion-getter-pump. The pressure which can be reached with this system is typically of the order of 10^{-4} Pa.

As can be seen from the experimental points in Fig. 9 the combined effect of traces of residual oxygen, other unknown impurities present and radiation products accumulated as a result of the repetitive character of the measurement, is of the same order as the effect of 10^{-6} M oxygen. This did

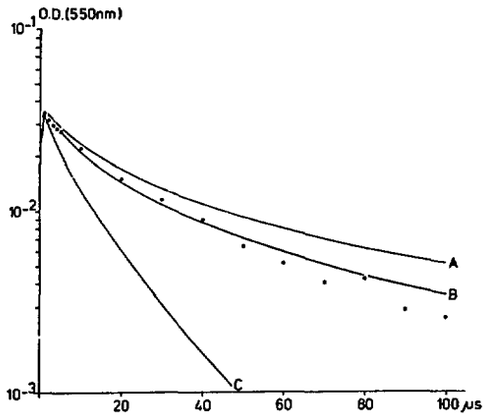

Fig. 9 Calculated decay of the hydrated electron. A: decay without oxygen; B: concentration of oxygen = 10^{-6} M; C: concentration of oxygen = 5 x 10^{-6} M. The dots represent the experimental points, obtained with a solution containing 0.5% n-butanol at pH = 11.5 using NaOH and deaerated as well as possible with the freeze-thawing technique.

not interfere with the experiments.

2.8 Performance

The precision of this system is determined by two factors, the first consists of the different types of noise [1], the other is the pulse to pulse reproducibility of the linac.

Complications of the first type are shot noise, current variations of the lamp power supply, physical movements of the arc and vibrations of the optical system. Of minor importance [1] are the types of noise produced in the amplifiers and the noise on the dark current. Shot noise results from the statistical characteristics of the photo-electrons generated in the detector and is determined by the rise time of the electronic system and thereby in our system by the

sample width of 800 ns (fixed). The system used to improve the problems arising from the current variations of the power supply of the lamp has been described before. The mechanical problems were solved by a more sturdy design such as the construction of the lamp cooling system.

The second factor is the pulse-to-pulse reproducibility of the accelerator beam because of the repetitive character of the measurements. Pulse monitoring was not done, because the toroid current monitor did not function satisfactory in this environment.

In practice it is difficult to discriminate between these effects. The point of interest, however, is the precision experimentally achieved. Therefore it was decided to test the performance experimentally on systems which are well known and trusted. To this end we have selected the e^-_{aq} system (to test the spectral characteristics) and the $(CNS)_2^-$ system (to test the time resolution), as will be described below.

2.8.1 The e^-_{aq} system

The absorption spectrum of the hydrated electron has been investigated on numerous occasions [10-13]. We measured the spectrum of e^-_{aq} in a solution of 0.5% n-butanol in water at pH = 11.5.

Figure 10 shows the spectrum at a dose of 7.7 Gy. The experimental conditions were: apparent time interval between the samples of the signal 1 µs, 128 electron bursts per measurement (2 complete measuring cycles).

Figure 11 displays the spectrum at a dose approximately 50 times smaller. Here the experimental conditions were: apparent interval 4 µs, 1008 bursts per measurement (63 measuring cycles). The represented points are calculated in both cases by extrapolating to the end of the electron burst by means of the KLPP program.

The measurements were performed with deaerated solutions and a lightpath of 1 cm. The spectra obtained are in

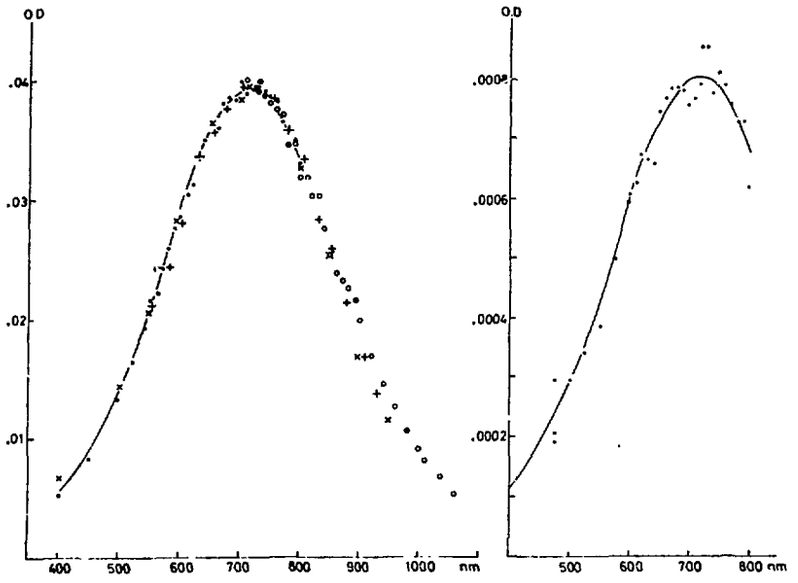

Fig. 10 Absorption spectrum of the hydrated electron, 1 cm lightpath, dose is 7.7 Gy.
- : J.P. Keene (1964); x : S. Gordon and E.J. Hart (1964); + : U. Schindewolf, H. Kohrmann and G. Lang (1969), see refs. [10-13]; · : experimental points (grating 33-86-02); o : experimental points (grating 33-86-03). The values of the literature are corrected for the dose.

Fig. 11 Absorption spectrum of the hydrated electron, 1 cm lightpath, dose is 0.15 Gy.
- : J.P. Keene (1964); · : experimental points.

excellent agreement with the literature values as given in the same figure.

The slight structure in the spectrum around 840 nm displayed in Fig. 10 is an artefact due to the limited slit width of the monochromator in combination with the occurrence of two narrow peaks in the spectrum of the Xenon-arc lamp.

2.8.2 The $(CNS)_2^-$ system

The radiolysis of potassium thiocyanate solutions has been investigated by several authors [14,15,16]. Under the conditions to be described, the following set of reactions apply [16].

$$OH\cdot + CNS^- \rightarrow CNSOH^- \qquad k_1 = 2.8 \times 10^{10}\ M^{-1}.sec^{-1} \qquad (1)$$

$$CNSOH^- \underset{k_{-2}}{\overset{k_2}{\rightleftarrows}} CNS\cdot + OH^- \qquad k_2 > 5 \times 10^7\ sec^{-1} \qquad (2)$$

$$CNS\cdot + CNS^- \underset{k_{-3}}{\overset{k_3}{\rightleftarrows}} (CNS)_2^- \qquad k_3 = 6.8 \times 10^9\ M^{-1}.sec^{-1},\quad k_{-3} = 3.4 \times 10^4\ sec^{-1} \qquad (3)$$

In the presence of N_2O the yield of OH· and therefore of $(CNS)_2^-$ is enhanced due to the reaction:

$$e^-_{aq} + N_2O \rightarrow N_2 + OH\cdot + OH^- \qquad (4)$$

The $(CNS)_2^-$ ion is a transient with a strong absorption band around 475 nm. Under the experimental conditions (4×10^{-5} M KCNS, pH = 6 buffered by means of a phosphate buffer, deaerated and N_2O added) the increase is described by [16]:

$$\frac{O.D._{eq} - O.D._t}{O.D._0} = \frac{-k_3[CNS^-]}{(k_1[CNS^-]-k_3[CNS^-]-k_{-3})}\, e^{-k_1[CNS^-]t} + \frac{k_3k_1[CNS^-]^2}{(k_3[CNS^-]+k_{-3})(k_1[CNS^-]-k_3[CNS^-]-k_{-3})}\, e^{-(k_3[CNS^-]+k_{-3})t}$$

$$= -0.034\ e^{-1.12 \times 10^6\ t} + 0.818\ e^{-3.06 \times 10^5\ t}$$

In this formula $O.D._t$ and $O.D._{eq}$ are the optical densities at time t and at equilibrium. $O.D._0$ is the optical density which would be attained if all the ·OH-radicals were converted to $(CNS)_2^-$ through the forward reaction 3.

After 2 μs the first term can be neglected and the rate of the increase is gouverned by the second term. A plot

of ($O.D._{eq}$ - $O.D._t$) versus time on a semi-logarithmic scale should show a straight line from which a half-life of 2.27 μs can be calculated. The half-life observed in Fig. 12 is 2.10 μs. The error is approximately 13%, originating to a great extent from the time uncertainty of 0.5 μs between the attention pulse from the linac and the 1 MHz clock of the sampling system.

Other systems to be described in the following chapters with half-lives on the micro-second time scale also show good agreement with literature data where available.

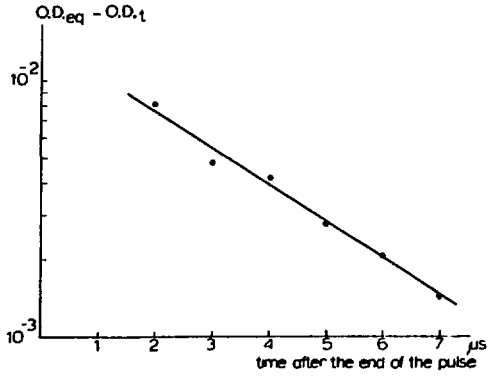

Fig. 12 Semi-logarithmic plot showing the increase of the $(CNS)_2^-$ radical (475 nm).
$O.D._{eq}$: optical density at equilibrium
$O.D._t$: actual optical density at time t.

2.8.3 Sensitivity

The spectrum displayed in Fig. 11 deserves a more detailed comment. From the scatter in the data points in this figure a judgement can be made of the overall sensitivity compared with conventional systems such as described and analyzed by J.P. Keene [1,17]. When the sensitivity is defined as that O.D. which is equal to the scatter in the data points, the sensitivity around 600 nm is about 5×10^{-5}. This was achieved under the following conditions: i) photocurrent: ca. 24 μA (60 μA light power on the detector), ii) bandwidth of the monochromator: 10 nm, iii) 63 measuring cycles used. This was a typical experiment.

Further improvement of the sensitivity can be achieved by increasing the bandwidth of the monochromator, by increasing the number of mea uring cycles or by optimizing the components of the optical system to the 1 cm cell used by us.

Keene describes [1] a system using a photomultiplier (cathode current: 10 μA, risetime of the amplification system: 1 μsec, bandwidth of the monochromator: 50 nm). In Keene's system only the sensitivity resulting from the shot-noise is considered and is similar to the sensitivity achieved with the experiment described above. Shot-noise is determined by the photo-current and the risetime of the amplifier [1]. The risetime of 1 μsec compares with the sample time of 800 nsec of our digitizing system.

One may conclude that both systems have comparable sensitivities. However, our experiment has a better spectral resolution (10 nm vs. 50 nm bandwidth). Furthermore it will be difficult to obtain a linear response from the photomultiplier system with a cathode-current of 10 μA [1,17].

2.9 Dosimetry

Both systems treated in section 2.8 are used as pulse dosimeters [18].

A comparison was made between the e^-_{aq} dosimeter and the aerated $(CNS)^-_2$ dosimeter without N_2O. At the doses used (smaller than 15 Gy/pulse) the results were in agreement within the experimental error. In the investigations described in the next chapters, the e^-_{aq} dosimeter was used,

The e^-_{aq} dosimeter solution consisted of a deaerated solution of 0.5% n-butanol at pH = 11.5. The $(CNS)^-_2$ dosimeter was a solution of 10^{-2} M at pH = 6 (phosphate-buffer) in an open vial.

The dose can be represented as:

$$\text{Dose (Gy)} = \frac{D \times 9.64 \times 10^6}{G \times \varepsilon \times l} \qquad 18)$$

D = optical density, G = yield/100 eV, ε = extinction-

coefficient of the absorbing species and l = length of the lightpath used, in this case l = 1 cm.

In the calculations the following numerical values were used:

e^-_{aq} : G = 2.63 and ε(715 nm) = 1.85 x 10^4 $M^{-1}cm^{-1}$ [19]
From these figures and our measured absorption spectrum are calculated: G x ε(550 nm) = 2.5 x 10^4 and G x ε(600 nm) = 3.5 x 10^4.

$(CNS)^-_2$: G(OH) = 2.72 [19] and ε($(CNS)^-_2$, 475 nm) = 7.6 x 10^3 $M^{-1}cm^{-1}$ [16].
G x ε(475 nm) = 2.07 x 10^4.

In all cases the optical density immediately after the pulse was determined by extrapolation by means of the KLPP program.

References

1) J.P. Keene, Proc. Int. Symp. on Pulse-Radiolysis, Manchester (1965) 1

2) L.M. Dorfman, M.S. Matheson, Progress in Reaction Kinetics, Vol. III. Ed. G. Porter (1965)237 (Pergamon Press)

3) M.C. Sauer, Jr., Argonne National Laboratories, ANL-7113 (1963)

4) C.G. Hobaugh, L.K. Patterson, R.W. Fessenden, Radiation Research Laboratories, Mellon Institute of Science, Carnegie-Mellon University, SR-16 (1973)

5) P.J.T. Bruinsma, J.J. Noomen and C. de Vries, Nucl. Instr. Meth. 74 (1969) 1

6) R.G. Alsmiller, Jr., J. Barish and S.R. Dodge, Nucl. Instr. Meth. 121 (1974) 161

7) W.A. Seddon, E.B. Selkirk and J.W. Fletcher, Int. J. Rad. Phys. Chem. 5 (1973) 323

8) K.H. Schmidt, Argonne National Laboratories, ANL-7199 (1966)

9) D.F. Detar, Computer Programs for Chemistry, Vol. 3, W.A. Benjamin, Inc. (1969)

10) J.P. Keene, Rad. Res. 22 (1964) 1

11) S. Gordon and E.J. Hart, J. Amer. Chem. Soc. 86 (1964) 5343

12) E.J. Hart and M. Anbar, The Hydrated Electron, Wiley Interscience, London (1970) 41

13) U. Schindewolf, H. Kohrmann and G. Lang, Angew. Chem, Intern. Ed. Engl. 8 (1969) 512

14) J.H. Baxendale and D.A. Stott, Chem. Comm. 14 (1967) 699

15) J.H. Baxendale, P.L.T. Bevan and D.A. Stott, Trans. Faraday Soc. 64 (1968) 2389

16) D. Behar, P.L.T. Bevan and G. Scholes, J. Phys. Chem. 76 (1972) 1537

17) J.P. Keene, J. Sci. Instr. 41 (1964) 493

18) N.W. Holm and R.J. Berry, Manual on Radiation Dosimetry, Marcel Dekker, Inc., New York (1970) 100

19) E.J. Hart, Rad. Res. Rev. 3 (1972) 285

CHAPTER III

SOME ASPECTS OF THE RADIOLYSIS OF METAL COMPLEXES IN THE PRESENCE OF ALCOHOLS

3.1 Introduction

At least in its earlier stages the radiolysis of diluted solutions in water can be described by the reactions of the primary species with the solutes, cf. section 1.2. The reaction of one of these species, the solvated electron, with metal complexes was introduced in section 1.3. In the present chapter the general aspects of the radiolysis of metal complexes in the presence of alcohols will be treated. The alcohols are necessary in order to minimize the interference of the most abundant primary species other than e^-_{aq}: ($OH^\cdot$ and $H^\cdot$):

$$OH^\cdot + RHOHCH \rightarrow H_2O + RHOHC^\cdot \qquad (1)$$

$$H^\cdot + RHOHCH \rightarrow H_2 + RHOHC^\cdot \qquad (2)$$

R = aliphatic part of the alcohol molecule.
In the presence of oxygen the HO_2 radical is generated, which is a powerful oxidant. In addition the hydrated electron reacts with oxygen at a diffusion controlled rate. In order to suppress these interferences all solutions to be irradiated have to be deaerated.

The investigations described in this thesis deal with octahedric complexes of metals with predominantly EDTA. In order to compare these EDTA complexes with the available data for hydrated metal ions, the latter ones will also be described as complexes: $M(H_2O)_6^{2+}$. In our work the reaction of hydrated electrons and metal complexes can be described by:

$$e^-_{aq} + M(II)L_6 \rightarrow M(I)L_6 \qquad (3)$$

M = any metal able to form complexes

L_6 = ligand sphere of the complex, e.g. $(H_2O)_6$, EDTA,... .

The fate of the reduced metal complex can be studied by investigating the factors which influence the decay of this complex when it has an absorption spectrum (Chapter VI) or by investigating the products formed from this complex if those have an absorption spectrum (Chapter V). The decay of the reduced metal complex consists of:

i) Oxidation by H_2O_2 [1,2] present as primary species:

$$M(I)L_6 + H_2O_2 \rightarrow M(II)L_6 + OH\cdot + OH^- \qquad (4)$$

ii) Dismutation or combination [3,4]:

$$2\ M(I)L_6 \rightarrow M(0)L_n + M(II)L_6 + (6-n)L \qquad (5a)$$

$$2\ M(I)L_6 \rightarrow M_2L_n + (12-n)L \qquad (5b)$$

iii) Reaction with the alcohol radical [3-7] formed by reactions (1) and (2):

$$RHOHC\cdot + M(I)L_6 \rightarrow RHOHCM(II)L_5 + L \qquad (6)$$

The radiolysis of metal complexes is described by reactions (1) - (6). The reactions (1) - (3) and (6) will be discussed further in the next sections, reaction (4) in Chapter VI. In the systems we studied, reactions (5a) and (5b) were of no consequence.

5.2 *The reaction with the hydrated electron*

The rate constant of reaction (3) is very large in many cases [8] when the ligand is water. Some of the factors influencing the rate constant are treated in section 1.3. In the case of the ligand being water the reduced complex often has a very intense absorption around 300 nm [8]. This absorption has been assigned to a charge transfer transition, because of the high extinction coefficient [8] and the possibility of photolyzing $M(I)(H_2O)_6^+$ solutions at 300 nm, yielding solvated electrons [9].

Other octahedric complexes which have been studied involve Ni(II), Cd(II), Zn(II), Al(III), Pb(II) and Cu(II) complexed by EDTA, NTA (nitrilo acetic acid), ethylene diamine and glycine [10]. Furthermore the rate constant of reaction (3) has been measured by Anbar *et al.* [11] for a large number of EDTA complexes.

Little is known about the absorption spectra of the reduced metal complexes when the ligand is not water. Meyerstein *et al.* [12] reported that Cd(I) complexed with ethylene diamine, glycine, NTA or EDTA absorbs around 320 nm. The absorption spectra of some reduced EDTA complexes will be discussed further in the Chapters IV and VI.

3.3 Reactions of the primary species H· and OH· with the alcohol

The abstraction of a H-atom from an alcohol (reactions (1) and (2) is most probable on the alpha-position [13] if possible (Table 1). The alcohol alpha-radical formed is a stronger acid than the original alcohol [13]:

$$RH(OH)C\cdot + OH^- \rightleftarrows [RH(O)C\cdot]^- + H_2O \qquad (7)$$

This equilibrium has a pK_a of 10.5 - 12 (Table 1) and is reached very fast (probably diffusion controlled [14]).

The alpha-radicals disappear by combination or disproportionation [15]:

$$RHOHC\cdot + RHOHC\cdot \rightarrow (RHOHC)_2 \qquad (8a)$$

$$RHOHC\cdot + RHOHC\cdot \rightarrow RHCO + RHOHCH \qquad (8b)$$

The rate of disappearance for the anionic forms of the alpha-radicals through reactions similar to (8a) and (8b) is about a factor 3 slower than that of the corresponding neutral forms (Table 1).

Table 1 Reaction rates ($M^{-1}s^{-1}$) for the H-abstraction by H· radicals (k_1) and OH· radicals (k_2) from alcohols; properties of the reaction products

Alcohol	$k_1 \times 10^{-9}$ 16)	$k_2 \times 10^{-7}$ 17)	% attack at α-carbon 12)	pK_a 14)	$k_8 \times 10^{-9}$ 15) neutral forms	$k_8 \times 10^{-9}$ 15) anionic forms
Methanol	0.84	0.2	100	10.7	2.4	0.9
Ethanol	1.8	2	97	11.6	2.3	0.5
n-Propanol	2.7	3	61	11.5		
2-Propanol	2.0	8	89	12.2	1.4	0.4
n-Butanol	4.0	3.8	34	11.5	∿ 1	
2-Butanol	3.5	10	75	11.6	∿ 1	
t-Butanol	0.54	0.01	-	-	1.3	

3.4 *The reaction of the alcohol radical with the (reduced) metal complex*

The purpose of adding alcohol to the reaction mixture is to convert the OH· and H· radicals into products which interfere less with the reactions of the hydrated electron. To play a significant role in the reaction scheme of the products of the reactions of the hydrated electron, these products should have reaction rates of at least the same order of magnitude as the other reactions involved (e.g. reactions (4), (5) and (8)). These latter rates are of the order of 10^9 $M^{-1}s^{-1}$ (Table 1).

In the case of the hydrated metal ions reaction (6) and the spectrum of the product of reaction (6) were reported for M = Zn [4], M = Co [4], M = Cd [3,4], M = Ni [5] and M = Cr [6,7]. These data are compiled in Table 2 for a series of organic OH· scavengers.

The occurrence of reaction (6) for EDTA complexes of copper and cadmium will be discussed in the Chapters V and VI. These cases are in fact postulated as analogues of the cases of the water complexed metals, because Schwarzenbach *et al.* have demonstrated that metal-EDTA complexes are often 5-coordinated by the EDTA and possess an additional H_2O or OH^--ligand [18,19]. This H_2O-ligand can be replaced by e.g. ammonia, thiocyanate, cyanide or ethylene-diammine with the same ease as in ordinary aquo-complexes. This information leads to the expectation that reaction (6) can also be observed with EDTA complexes.

In the case of t-butanol the reaction with OH· radicals is capable only of producing beta-radicals. These beta-radicals can also yield metal-carbon complexes as can be seen in Table 2, but one has to consider the possibility of reaction (9) [3]:

$$M^+ + (CH_3)_2C(\dot{C}H_2)OH \rightarrow M^{2+} + (CH_3)_2C=CH_2 + OH^- \qquad (9)$$

Reaction (9) has been postulated for Cd^+ and Ni^+ [3,5]. Neglecting reaction (9) could possibly result in overestimating k_6 and underestimating the absorption coefficients measured.

Table 2 Rate of formation ($M^{-1}s^{-1}$) of the metal-carbon complexes from water complexed metals and their absorption maximum (nm). Compiled from references [3-7]

	formate		methanol		ethanol	
	k_6	λ_{max}	k_6	λ_{max}	k_6	λ_{max}
Cr^{2+}			1.6×10^{8}	282	7.9×10^{7}	296
Ni^{+}	6.6×10^{9}	<250	4.2×10^{9}	<250	3×10^{9}	270
Cd^{+}	$(1-5)\times10^{9}$	<250	2×10^{8}	<250	1.3×10^{9}	
Co^{+}	$(1-5)\times10^{9}$	<250	$(1-5)\times10^{9}$	<250		
Zn^{+}	$(1-5)\times10^{9}$	290	$(1-5)\times10^{9}$	295		

	2-propanol		t-butanol		ethoxy-ethane	
	k_6	λ_{max}	k_6	λ_{max}	k_6	λ_{max}
Cr^{2+}	5.1×10^{7}	311	1.0×10^{8}	310	3.4×10^{7}	291
Ni^{+}	1.4×10^{9}	<250			0.8×10^{9}	290
Cd^{+}	2.4×10^{9}	<250	$(1-5)\times10^{9}$	<250		
Co^{+}	$(1-5)\times10^{9}$	<250	$(1-5)\times10^{9}$	<250		
Zn^{+}	$(1-5)\times10^{9}$	305	$(1-5)\times10^{9}$	300		

References

1) D. Meyerstein and W.A. Mulac, J. Phys. Chem. 72 (1968) 784

2) G.V. Buxton, R.B. Sellers and D.R. McCracken, J. Chem. Soc., Far. Trans. I, 72 (1976) 1464

3) M. Kelm, J. Lilie and A. Henglein, J. Chem. Soc. 75 (1975) 1132

4) G.V. Buxton and R.B. Sellers, J. Chem. Soc., Far. Trans. I, 71 (1975) 558

5) M. Kelm, J. Lilie, A. Henglein and E. Janata, J. Phys. Chem. 78 (1974) 882

6) W. Schmidt, J.H. Swinehart and H. Taube, J.A.C.S. 93 (1971) 1117

7) H. Cohen and D. Meyerstein, Inorg. Chem. 13 (1974) 2434

8) J.H. Baxendale, E.M. Fielden and J.P. Keene, Proc. Roy. Soc., Ser. A, 286 (1965) 320

9) N. Basco, S.K. Vidyarthi and D.C. Walker, Can. J. Chem. 52 (1974) 343

10) E.J. Hart and M. Anbar, The Hydrated Electron, Wiley-Interscience, New York (1970) 117

11) M. Anbar and D. Meyerstein, Trans. Far. Soc. 65 (1969) 1812

12) D. Meyerstein and W.A. Mulac, Inorg. Chem. 9 (1970) 1762

13) G.E.D. Adams and R.L. Willson, Trans. Far. Soc. 65 (1969) 2981

14) K.-D. Asmus, A. Henglein, A. Wigger and G. Beck, Ber. Bunsenges.Phys. Chem. 70 (1966) 756

15) M. Simic, P. Neta and E. Hayon, J. Phys. Chem. 73 (1969) 3794

16) L.M. Dorfman and G.E. Adams, NSRDS-NBS 46 (1973)

17) M. Anbar, Farhataziz and A.B. Ross, NSRDS-NBS 51 (1975)

18) G. Schwarzenbach and H. Ackermann, Helv. Chim. Acta 30 (1947) 1798

19) G. Schwarzenbach, Helv. Chim. Acta 32 (1949) 839

CHAPTER IV

SOME ASPECTS OF SOLVATED ELECTRON REACTIONS

4.1 Introduction

One of the initial steps in the reaction schemes discussed in the next two chapters is the reaction of the solvated electron with a metal-EDTA complex [1,2]

$$e^-_{aq} + MEDTA^{2-} \rightarrow \text{products} \qquad (1)$$

In the cases discussed here these products are reduced metal-EDTA complexes. In general the rate of reaction 1 is one or two orders of magnitude smaller than the reaction of the solvated electron with the corresponding aquo-complexes, as published by Anbar *et al.* [2]. These measurements were performed at a rather high ionic strength. We decided therefore to repeat some of these measurements at lower ionic strengths.

To make sure that the metals were fully complexed by the EDTA, an excess of this reagent was present, but this excess did not exceed 10 percent. This situation made it necessary to investigate the possibility of an interference by the reaction:

$$e^-_{aq} + EDTA \rightarrow \text{products} \qquad (2)$$

As will be shown reaction 2 did never seriously interfere at the pH used for the other measurements (pH = 11.5).

Among the primary species other than e^-_{aq} OH·, H· and H_2O_2 are relevant. OH· and H· are scavenged by n-butanol (60 mM):

$$OH\cdot + RHOHCH \rightarrow RHOHC\cdot + H_2O \quad k_3 = 4 \times 10^9\ M^{-1}s^{-1}\ 3) \qquad (3)$$

$$H\cdot + RHOHCH \rightarrow RHOHC\cdot + H_2 \quad k_4 = 3.8 \times 10^7\ M^{-1}s^{-1}\ 4) \qquad (4)$$

At the doses used H_2O_2 will reoxidize the reduced metal-EDTA complexes formed by reaction 1 [5,6] on a millisecond time scale or even more slowly.

4.2 *Experimental*

The composition of the samples used for the determination of the rate constant k_1 was a solution of 60 mM n-butanol in water adjusted to a pH of 11.5 by means of NaOH and such a concentration of the substrate that the half-life of the solvated electrons measured was between 1 and 7 μs. The excess of Na_2H_2EDTA in these samples was ≤ 1 mM. In addition some of the experiments were performed with 60 mM methanol instead of n-butanol as OH· scavenger.

The samples used for the determination of k_2 consisted of the same solution to which either 5 mM phosphate, borax or carbonate were added in order to buffer the solutions to the pH desired. The concentration of EDTA was such that the half-life of the solvated electrons was between 1 and 7 μs.

The doses were between 5 and 10 Gy. The rate constants obtained were corrected for the competing reaction of the solvated electron with the other solutes. The purity of the chemicals and the water was as described in Chapter II. Especially for the measurements of k_2 it was important to recrystallize the Na_2H_2EDTA carefully, in order to suppress the reactions of the solvated electrons with impurities.

4.3 *The reaction of the solvated electron with EDTA*

The rate of reaction 2, which is quoted by Anbar *et al.* as $k_2 < 1.5 \times 10^6\ M^{-1}s^{-1}$, $8 < pH < 11$ [7], is expected to depend on the pH, because all the functional groups of EDTA (ethylene-diammine-tetra-acetic acid) are subject to acid-base equilibria. The most important acid-base equilibrium constants are: $pK_1 = 2.0$, $pK_2 = 2.7$, $pK_3 = 6,2$ and $pK_4 = 10.3$ [8]. These values suggest that H_4EDTA has the structure of a zwitterion:

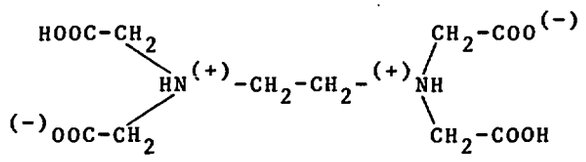

The protons attached to the N-atoms are associated with pK_3 and pK_4 [8]. Since we studied the pH region between 6 and 11.5, the influence of the pH is attributed to these protons, and variations in the rate constant k_2 are expected around pH 6.2 and 10.3.

The results of the measurements of k_2 at a total ionic strength $\mu = 0.12$ are shown in Figure 1 as a function of of the pH. The reaction rate k_2 can be considered as the total sum of the individual reaction rates of all the dissociation steps of EDTA with the solvated electron:

$$k_2 = k_2' f(EDTA^{4-}) + k_2'' f(HEDTA^{3-}) + k_2''' f(H_2EDTA^{2-}) + \ldots$$

In this equation the meaning of the symbol f is: the fraction of the ions quoted in parentheses at that particular pH. For k_2' is very small, $k_2'' = 4.7 \times 10^6$ and $k_2''' = 1.0 \times 10^8\ M^{-1}s^{-1}$, the solid line shown in Figure 1 is obtained. Above pH = 10 no experimental points can be measured at this total ionic strength, because the reaction becomes too slow compared with the other reactions of e^-_{aq}. Increasing the concentration of the EDTA has the result that the total ionic strength becomes larger than 0.12. We performed some experiments at a larger ionic strength which yield:

i) pH = 11.1, μ = 1.6: $k_2 = 1.1 \times 10^6\ M^{-1}s^{-1}$,
ii) pH = 11.5, μ = 1.6: $k_2 \sim 4 \times 10^5\ M^{-1}s^{-1}$.

These values indicate that the scheme is correct and that the value of k_2' is small indeed.

The total ionic strength can be varied by the addition of an inert salt (Na_2SO_4). From the variation of the reaction rate with the ionic strength, information can be obtained concerning the sign of the charges of the species involved and an indication of the value of the charges according

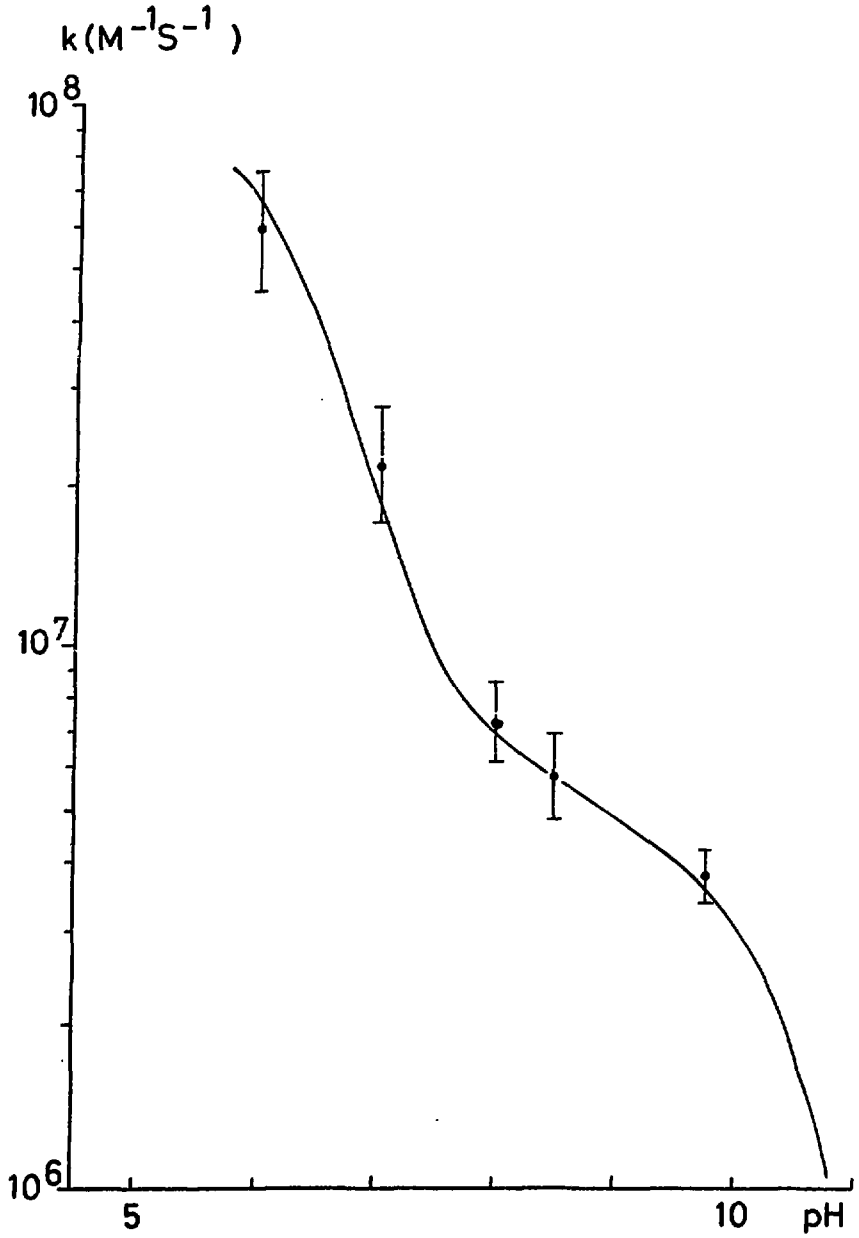

Fig. 1 Variation of $k(e^-_{aq}$ + EDTA) with pH at a total ionic strength $\mu = 0.12$. The solid line represents the rate constant calculated from: $k_2 = 4.7 \times 10^6$ x (fraction of $HEDTA^{3-}$) + 1.0×10^8 x (fraction of H_2EDTA^{2-})

to the Debye-Hückel theory [9]. We performed such experiments between pH = 6.5 and pH = 8.5. In this range the reaction of H_2EDTA^{2-} with e^-_{aq} is the most important one. We found: $Z(e^-_{aq}) \times Z(H_2EDTA^{2-}) = 0.8 \pm 0.3$ for a reaction radius of 3 Å (which is too small, but often taken for convenience) or 1.5 ± 0.5 for a reaction radius of 6 Å. These values are rather low, which may be explained by the rather long distances between the positions of the charges in the molecule and the reaction site.

The mechanism of reaction 2 is probably the acid catalized conversion of solvated electrons into H· radicals [10]:

$$e^-_{aq} + HA \rightarrow H\cdot + A^- \qquad (5)$$

HA stands for any acid. According to the Brönsted theory a plot of k_5 against pK_a should yield a straight line [11], as shown in Figure 2 for formic acid, acetic acid, $H_2PO_4^-$ and NH_4^+. Also shown in this figure are the points corresponding to k_2'' and k_2''' ($HEDTA^{3-}$ respectively H_2EDTA^{2-}). The values of k_2'' and k_2''' are taken a factor 2 lower than the values quoted earlier because Figure 2 is valid only for a total ionic strength $\mu = 0$. These values still seem to be rather high, which may be attributed to an incomplete correction for the ionic strength or to other reactions of the solvated electron with EDTA, e.g.:

$$e^-_{aq} + \begin{matrix} & & R_1 \\ & & \backslash \\ & & HN^{(+)}-R_2 \\ & & | \\ (-)OOC-CH_2 & & \end{matrix} \rightarrow {}^{(-)}OOC-H_2C\cdot + \begin{matrix} R_1 \\ | \\ H\underline{N}-R_2 \end{matrix} \qquad (6)$$

Reaction 6 is similar to the deamination of amino-acids by the solvated electron [12].

4.4 The reaction of the solvated electron with some metal-EDTA complexes

Anbar *et al.* [2] published an extensive survey of rate constants of solvated electron reactions of the type of reaction 1. These measurements were performed at a constant

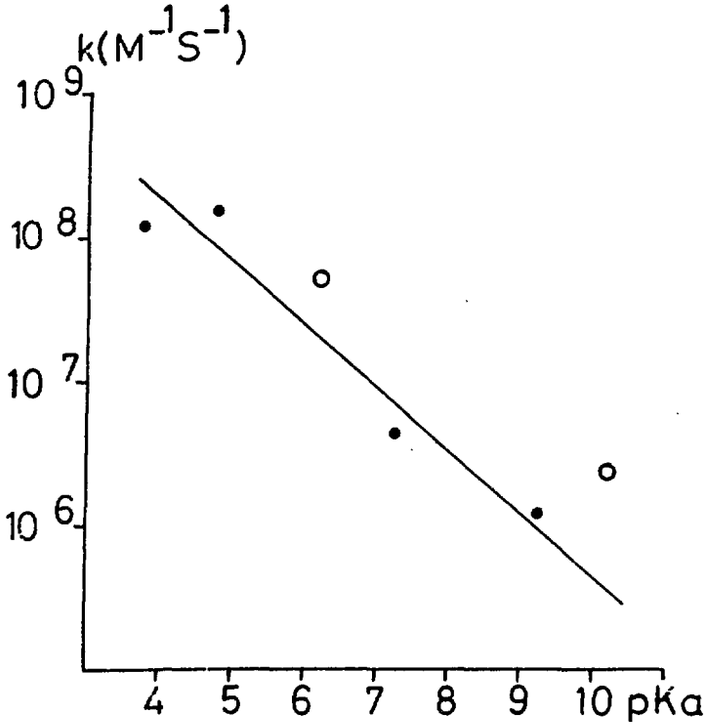

Fig. 2 Variation of $k(e^-_{aq} + S)$ with $pK_a(S)$. S (represented by a dot) is from left to right: formic acid, acetic acid, $H_2PO_4^-$ and NH_4^+. The symbol o corresponds to respectively H_2EDTA^{2-} and $HEDTA^{3-}$

ionic strength ($\mu = 0.2$), because there is an uncertainty in assigning the correct effective charge of the complexes because of hydrolysis according to [8]:

$$MEDTA^{n-} + OH^- \rightleftarrows M(OH)EDTA^{(n+1)-} \qquad (7)$$

Nevertheless, in practice one would like to perform experiments in which μ is not that high. In the cases we investigated and which will be discussed below, we did not find indications that the hydrolised forms of the complexes are very important. This was concluded from experiments in which the ionic strength was varied. In Figures 3 and 4 the variation of k_1 with $\sqrt{\mu}/(1+\sqrt{\mu})$ is shown. According to the Debye-

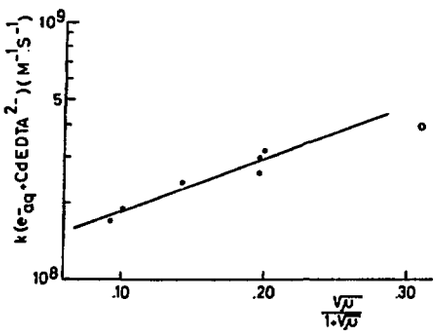

Fig. 3 Variation of $k(e^-_{aq} + CdEDTA^{2-})$ with the ionic strength (μ). •: experimental points, pH = 11.5, o: point taken from ref. [2], pH = 12. The solid line has a slope according to $Z(e^-_{aq}) \times Z(CdEDTA^{2-}) = +2$.

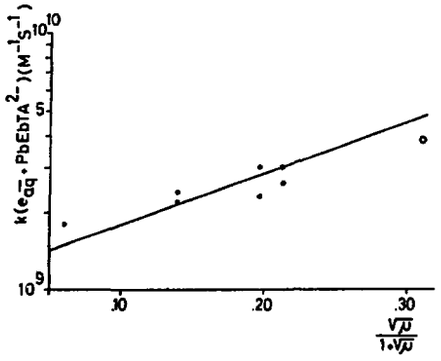

Fig. 4 Variation of $k(e^-_{aq} + PbEDTA^{2-})$ with the ionic strenght (μ). •: experimental points, pH = 11.5, o: point taken from ref. [2], pH = 12. The solid line has a slope according to $Z(e^-_{aq}) \times Z(PbEDTA^{2-}) = +2$.

Hückel theory [9] the points in these figures should be on a straight line. The straight lines in these figures have a slope corresponding to the charge of - 2 of the metal-EDTA complex and compare well with the experimental points.

The rate constants of the other metal-EDTA complexes measured by us are compared with the values of Anbar *et al.* [1,2] in Table 1. The value of k_1 at any ionic strength can be obtained from this table by interpolation between our values and the values from the literature, except for the case of Co(II) and Zn(II). In the case of Co(II) only an upper value is given because the amount of Co(III) present was uncertain. The value of Zn(II) was measured only at a high ionic strength because the rate constant is so small,

Table 1 Rates of reaction of e^-_{aq} with metal-EDTA complexes

metal	$\frac{\sqrt{\mu}}{1+\sqrt{\mu}}$	pH	$k(M^{-1}s^{-1})$	literature $\frac{\sqrt{\mu}}{1+\sqrt{\mu}}$	pH	$k(M^{-1}s^{-1})$	ref.
Cu(II)	0.08	11.5	6.5×10^9	0.31	12	1.04×10^{10}	2
Hg(II)	0.11	11.5	2.1×10^9	0.31	12	5.1×10^9	2
Co(II)	0.12	11.5	$\leq5.6\times10^8$*	0.31	12	$\leq5.2\times10^8$*	2
In(III)	0.12	11.5	2.3×10^8	0.31	12	4.1×10^8	2
Ni(II)	0.16	11.5	8.2×10^7	0.31	12	1.00×10^8	2
Ga(III)	0.15	11.5	4.7×10^7	0.31	11	7.8×10^7	2
Mn(II)	0.32	11.5	6.0×10^6	$\sim$0	11.3	1.5×10^6	1
Zn(II)	0.34	11.5	5.1×10^6	0.31	12	$\leq1.8\times10^6$	2

* Upper value due to an unknown amount of Co(III).

that we were compelled to use high concentrations in order to obtain an acceptable half-life for the e^-_{aq}. The precision of our values listed in Table 1 is about 15%.

The reduction of the water complexed metal ions by the solvated electron gives rise to products which often possess an intense absorption spectrum around 300 nm [13]. Also in the case of the metal-EDTA complexes investigated by us, we found that products of reaction 1 show U.V. absorption spectra. The absorption spectra of the reduced cadmium- and lead-complexes were measured best and will be discussed further in Chapter VI. Apart from the case of cadmium the absorption spectra do not show maxima above 300 nm. In these cases the absorption coefficient decreases gradually in the region from 300 to 400 nm. At 300 nm the absorption coefficients are approximately 3×10^3 $M^{-1}cm^{-1}$ for gallium and indium, 2×10^3 $M^{-1}cm^{-1}$ for cobalt and nickel and $< 2\times10^3$ $M^{-1}cm^{-1}$ for mercury and manganese.

References

1) M. Anbar and E.J. Hart, J. Phys. Chem. 71 (1967) 3700

2) M. Anbar and D. Meyerstein, Trans. Far. Soc. 65 (1969) 1812

3) L.M. Dorfman and G.E. Adams, NSRDS-NBS 46 (1973)

4) M. Anbar, Farhataziz and A.B. Ross, NSRDS-NBS 51 (1975)

5) D. Meyerstein and W.A. Mulac, J. Phys. Chem. 72 (1968) 784

6) G.V. Buxton, R.B. Sellers and D.R. McCracken, J. Chem. Soc.,Far. Trans. I, 72 (1976) 1464

7) M. Anbar, M. Bambenek and A.B. Ross, NSRDS-NBS 43 (1973)

8) G. Schwarzenbach and H. Ackermann, Helv. Chim. Acta 30 (1947) 1798

9) S. Glasstone, "Textbook of Physical Chemistry", MacMillan and Co., Ltd, London, pages 966 and 1115 (1955)

10) J.K. Thomas in "Advances in Radiation Chemistry", ed. M. Burton, J. Magee, Vol. 1, John Wiley and Sons, New York (1969) 157

11) R.P. Bell, "The Proton in Chemistry", Cornell University Press, Ithaca, (1959) 155

12) P. Neta, M. Simic and E. Hayon, J. Phys. Chem. 74 (1970) 1214

13) J.H. Baxendale, E.M. Fielden and J.P. Keene, Proc. Roy. Soc.,Ser. A, 286 (1965) 320

CHAPTER V

THE RADIOLYSIS OF $CuEDTA^{2-}$

5.1 *Introduction*

The radiation chemistry of hydrated cupric ions and complex cupric ions was described by Meyerstein [1,2]. In both cases the formation of Cu(I) and Cu(III)-states is observed. Degradation of (H-abstraction from) the EDTA-ligand by the OH• radical instead of oxydation to the Cu(III)-state was reported by Bhattacharyya *et al.* [3].

During measurements of reaction rate constants of e^-_{aq} reacting with various metal-EDTA complexes a transient species absorbing around 440 nm was observed by us when the metal was copper. Later it turned out that the presence of an organic OH• scavenger, e.g. an alcohol, was a necessary condition for the formation of this transient. Initially the alcohol (n-butanol) was used as a scavenger for the OH• and H• radicals formed:

$$RHOHCH + OH\cdot \rightarrow RHOHC\cdot + H_2O \qquad (1)$$

$$RHOHCH + H\cdot \rightarrow RHOHC\cdot + H_2 \qquad (2)$$

The primary radicals H• and OH• thus being scavenged from the system made it possible to study reaction 3:

$$Cu(II)EDTA^{2-} + e^-_{aq} \rightarrow Cu(I)EDTA^{3-} \qquad (3)$$

$Cu(I)^+_{aq}$, which is similar to the product of reaction 3, does not show a detectable absorption spectrum as reported by Basco *et al.* [4]. This fact and the considerations mentioned in Chapter III concerning the influence of alcohols in the radiolysis of metal-complexes indicate that the following reaction must occur:

$$RHOHC^{\cdot} + Cu(I)EDTA^{3-} \rightarrow RHOHCCu(II)EDTA^{3-} \qquad (4)$$

The product of reaction 4 absorbs strongly around 440 nm (RHOHCH = n-butanol). The formation and some of the properties of this product are the subjects of this chapter.

5.2 *Experimental*

Typically the irradiated solutions contained 1 mM $CuEDTA^{2-}$ and about 60 mM butanol-1, or the same amount of another alcohol for some of the experiments. The pH of these solutions was adjusted to either 11.5 or 7.5 (in the latter case 5 mM phosphate was added) by means of NaOH. All chemicals and the water used were of the quality mentioned in Chapter II.

The solutions were measured with an apparent time sample interval of 8 μs. The number of measuring cycles varied between 1 and 3, in order to keep the radiolytic decomposition of the mixture at a minimum level. The dose per experiment varied between 5 and 10 Gy, giving an optical density in the 1 cm cuvette of 0.01 or less, as described in the next sections.

Figure 1 shows an example of an absorption spectrum of the transient species formed. The time needed for the formation of half the final yield of the transients was of the order of 50 μs.

5.3 *Spectral properties*

In Figure 2 the absorption spectrum is shown of copper complexed with EDTA and the radical formed from methanol, ethanol or butanol-1. One can see a shift of the absorption maximum to larger wavelengths as the alcohol molecule becomes larger. This indicates clearly that a constituent part of the absorbing species originates from the alcohol.

It is well known that $OH^{\cdot}$ and $H^{\cdot}$ radicals attack the alcohol preferably at the alpha-position [5], as mentioned in Chapter III. To investigate the relevance of this position

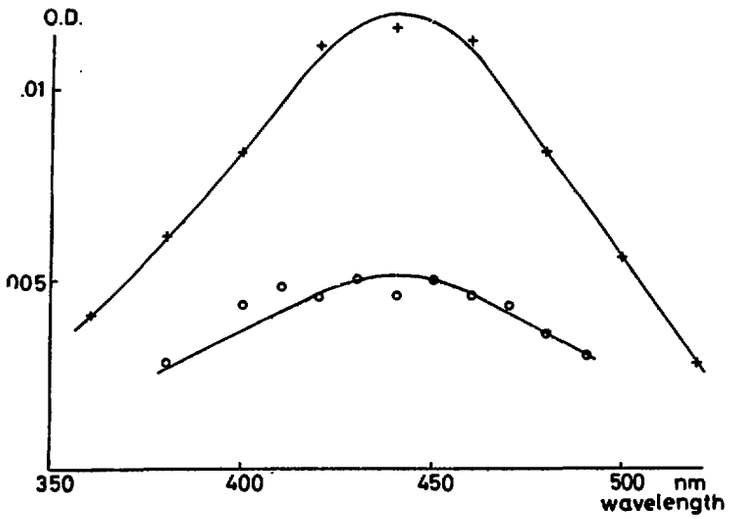

Fig. 1 Absorption spectrum of $CH_3(CH_2)_2HOHCCu(II)EDTA^{3-}$. +: pH = 8.5 (borax buffer). This spectrum does not differ from the spectra measured at pH = 7.5 or 7.0 (phosphate buffer); o: pH = 11.5

with respect to the formation of the transient we performed an experiment in which the alcohol was t-butanol, which only yields beta-radicals. As discussed in Chapter III these beta-radicals do not only react similarly to reaction 4, but they may also give the product of reaction 5:

$$Cu(I)EDTA^{3-} + (CH_3)_2\dot{C}(CH_2)OH \rightarrow Cu(II)EDTA^{2-} + (CH_3)_2C = CH_2 + OH^- \quad (5)$$

Reactions similar to reaction 5 were postulated by Kelm *et al.* [6,7], of the type of reaction 4 by Buxton *et al.* [8] and Cohen *et al.* [9]. In our case reaction 4 is of relevance, because the product is observed by means of the absorption spectrum (Figure 2). The alcohol group can also be replaced by another functional group as shown in Figure 3, where the absorption spectrum is shown for n-butyraldehyde as a reactant in reaction 4 instead of the alcohol.

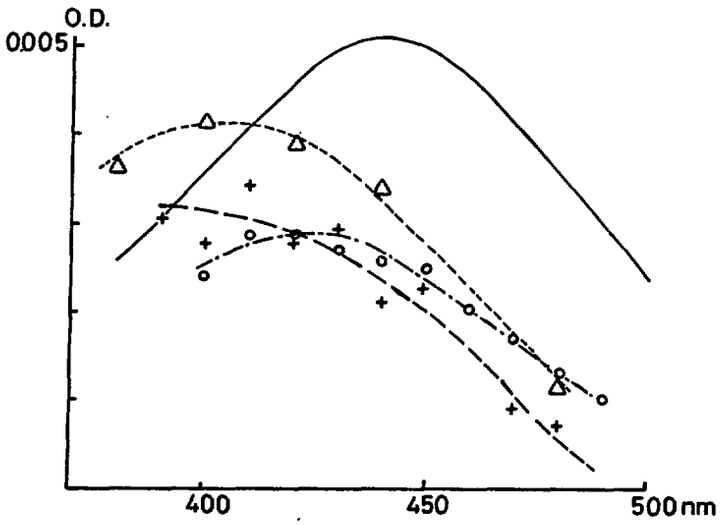

Fig. 2 Absorption spectrum of copper complexed with EDTA and the OH· scavenger product at pH = 11.5. OH· scavengers were: +: methanol; o: ethanol; Δ: t-butanol; solid line: n-butanol. The last spectrum is the average of more experiments.

EDTA is also part of the absorbing species as can be shown by replacing EDTA by CDTA (cyclohexylene diammine-tetra-acetic acid):

$$Cu(I)CDTA^{3-} + RHOHC\cdot \rightarrow RHOHCCu(II)CDTA^{3-} \qquad (6)$$

The absorption spectrum of the product of reaction 6 is shown in Figure 3 for RHOHCH = n-butanol. The absorption maximum of $RHOHCCuCDTA^{3-}$ is at a slightly but significantly longer wavelength than that of $RHOHCCuEDTA^{3-}$.

The formation of $RHOHCCuEDTA^{3-}$ requires a Cu-carbon bond to be formed. This bond has been discussed in Chapter III for the aqueous complexes of several metals (Table 2 of Chapter III). Schwarzenbach [10] has shown that $Cu(II)EDTA^{2-}$ is a penta-dentate EDTA complex with a H_2O molecule at the free position of the metal. This H_2O molecule can be exchanged by other ligands (ethylene diammine or

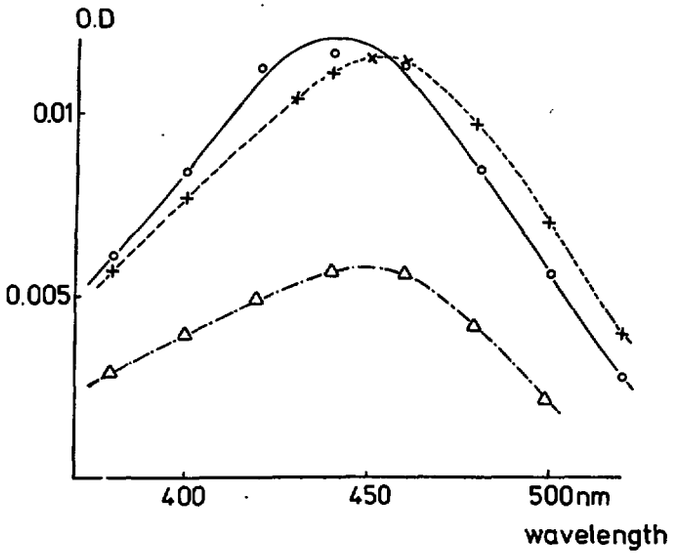

Fig. 3 Absorption spectrum of copper complexed with EDTA or CDTA and the OH· scavenger product.
o: OH· scavenger = n-butanol, EDTA, pH = 8.5 (borax buffer), the solid line is the average of more experiments; +: OH· scavenger = n-butanal, EDTA, pH = 7 (phosphate buffer); Δ: OH· scavenger = n-butanol, CDTA, pH = 7 (phosphate buffer).

CN^-) with the same ease as in the aqueous Cu(II) complex. If we assume that during reaction 3 the ligand-sphere remains intact and that during reaction 4 the H_2O-ligand is replaced by the (alcohol)radical, it is obvious that these Cu-carbon bonds are completely comparable to the metal-carbon bonds discussed in Chapter III.

The most complete series of metal-carbon bonds is described by Cohen and Meyerstein for chromium [9]. However, only little can be said about the similarity of the spectra of the copper compounds and the chromium compounds, because the former display only one absorption peak in the accessable wavelength interval. This absorption peak seems to correspond

to the large peak in the chromium compounds, which is attributed to a charge-transfer transition [9]. In both cases the nature of scavenger radical has a significant influence on the position of the absorption maximum (λ_{max}). In addition the molar absorption coefficients are large and the λ_{max} for RH = methanol is at the shortest wavelength, both of which are characteristics of charge-transfer transitions, c.f. [9].

5.4 Formation of the transient copper species

The time needed for the formation of half the final yield will be used frequently in the discussion. For this time we will use the symbol $T_{\frac{1}{2},f}$.

In the proposed mechanism for the formation of the transient species absorbing around 440 nm the important primary species of the radiolysis of water are e^-_{aq}, H· and OH·. H_2O_2 does not seem to play an important role, because Bhattacharyya *et al.* [3] found a final yield of H_2O_2 in deaerated solutions of Cu-EDTA complexes in agreement with the initial G-value. In this case no organic scavengers were present.

In our experiments organic scavengers were added to an amount sufficient to scavenge most OH· radicals, thus preventing the reaction of OH· with $Cu(II)EDTA^{2-}$ becoming important. For example, the alcohol which was mostly used, was n-butanol to a concentration of 60 mM. In this case the rate constant k_1 is 4.0×10^9 $M^{-1}s^{-1}$ [11]. The reaction of OH· with $Cu(II)EDTA^{2-}$ has a rate constant of about the same magnitude [3] *. The concentration of $Cu(II)EDTA^{2-}$ is at least six times smaller, however. From these values it is

* Bhattacharyya *et al.* found for $k(OH+CH_3OH)/k(OH+Cu(II)EDTA^{2-}) = 0.23$. Assuming $k(OH+CH_3OH) = 4.7 \times 10^8$ $M^{-1}s^{-1}$ they calculated $k(OH+Cu(II)EDTA^{2-}) = 2.0 \times 10^9$ $M^{-1}s^{-1}$. Using the commonly accepted value of 8.4×10^8 $M^{-1}s^{-1}$ for $k(OH+CH_3OH)$ [11] we calculated $k(OH+Cu(II)EDTA^{2-}) = 3.7 \times 10^9$ $M^{-1}s^{-1}$.

clear that most OH· radicals react through reaction 1.

The most probable reaction path for the H· radicals we considered to be reaction 2. For n-butanol, where $k_2 = 3.8 \times 10^7$ $M^{-1}s^{-1}$ [12], the half-life of the H· radicals is 0.3 μs at the concentrations used. However, it cannot be excluded that the H· radicals contribute to the formation of $Cu(I)EDTA^{3-}$ [3].

Reaction 3 has a rate constant k_3 equal to 6.5×10^9 $M^{-1}s^{-1}$ (Table 1, Chapter IV). The reactions discussed would lead to the conclusion that after a few μs only the following species can possibly produce the transient absorbing around 440 nm: $Cu(II)EDTA^{2-}$, $Cu(I)EDTA^{3-}$ (present with a yield equal to the primary yield of e^-_{aq}) and the alcohol radical (present with a yield equal to the sum of the primary yields of OH· and H·).

The evidence for the alcohol radical being a constituent part of this transient species is clear from the discussions in the previous section about the influence of the nature of the alcohol on the spectral properties of the transient. Additional evidence can be derived from Figure 4a where the yield of the transient is shown as a function of the OH· scavenger concentration (n-butanol). This behaviour can be understood if reaction 1 competes with the reaction of $Cu(II)EDTA^{2-}$ with OH·, while the alcohol radicals formed react in turn, yielding amongst others the transient species. If one assumes that an approximately constant fraction of the alcohol radicals formed yields the transient species one can derive:

$$\frac{O.D._{max}}{O.D.} = 1 + R\,\frac{[Cu(II)EDTA^{2-}]}{[butanol\text{-}1]} \qquad (I)$$

In this formula O.D. is the optical density, $O.D._{max}$ the optical density at high butanol concentrations and R the ratio of $k(Cu(II)EDTA^{2-} + OH\cdot)$ and k_1. The straight line in Figure 4b is derived from this formula and the experimental points from Figure 4a. From the tangent of this line, which corresponds to R, and the value of k_1, 4.0×10^9 $M^{-1}s^{-1}$ [11],

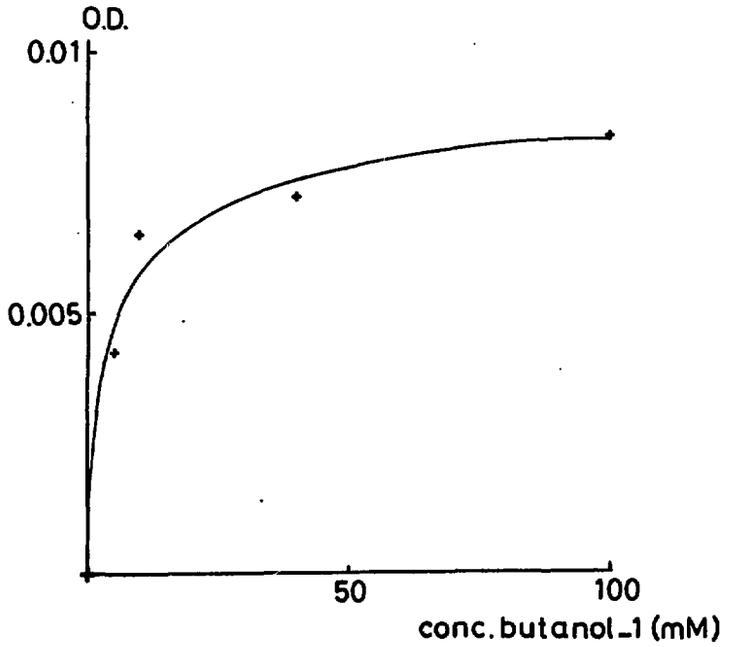

Fig. 4a Final O.D. at 440 nm of $CH_3(CH_2)_2HOHCCu(II)EDTA^{3-}$ as a function of the n-butanol concentration. The concentration of $Cu(II)EDTA^{2-}$ is 10 mM, pH is 7.5 (phosphate buffer).

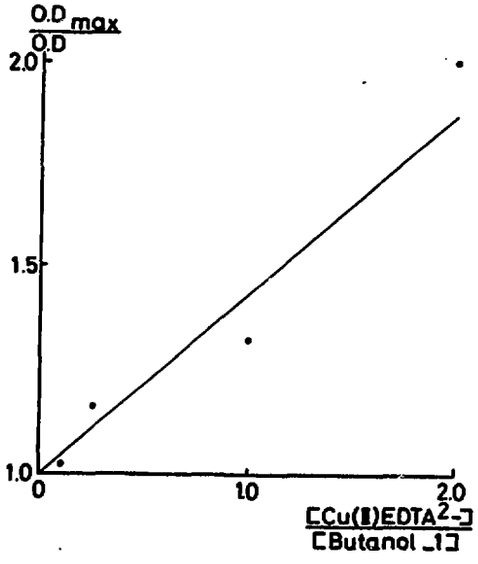

Fig. 4b The data from Figure 4a represented according to equation I, which describes the effect of the concurrent reactions of OH· with $Cu(II)EDTA^{2-}$ and n-butanol

we calculate: $k(Cu(II)EDTA^{2-} + OH\cdot) = 1.8 \times 10^9\ M^{-1}s^{-1}$. This agrees within a factor two with the value we calculated from the data of Bhattacharyya *et al.* [3]: $3.7 \times 10^9\ M^{-1}s^{-1}$.

It is the alcohol radical and not the alcohol itself which takes part in the formation reaction of the transient species because if it would be the alcohol itself, changing the alcohol concentration would change the rate of formation of the transient species in the same ratio. This is not the case: between 10 and 100 mM butanol-1 this rate changes very little.

The question remains with which copper compound the alcohol radicals react to yield the transient; the original $Cu(II)EDTA^{2-}$ or the $Cu(I)EDTA^{3-}$. In our opinion the formation reaction is reaction 4. It is postulated by Bhattacharyya *et al.* [3] that $Cu(II)EDTA^{2-}$ does react with the alcohol radicals, but they assume that this leads to the formation of $Cu(I)EDTA^{3-}$ and other products:

$$Cu(II)EDTA^{2-} + RHOHC\cdot \rightarrow Cu(I)EDTA^{3-} + \text{products} \qquad (7)$$

Furthermore, in the case of a reaction of the alcohol radicals with $Cu(II)EDTA^{2-}$ producing the transient, one would expect pseudo-first order kinetics, with a rate constant proportional to the concentration of the copper complex. However, experimentally it was found that, although the rate of formation did not increase, it did not do so proportional to the $Cu(II)EDTA^{2-}$ concentration. Increasing the concentration of the $Cu(II)EDTA^{2-}$ has also the effect of decreasing the yield of the transient as shown in Figure 5. This cannot be explained by competition of reaction 1 and the reaction of $OH\cdot$ with $Cu(II)EDTA^{2-}$, because the rate constant $k(Cu(II)EDTA^{2-} + OH\cdot)$ would then have to be larger than $8 \times 10^9\ M^{-1}s^{-1}$. This is more than twice the value calculated from [3], and four times the value found from Figure 4b. Furthermore, because reaction 1 is completed within less than a microsecond, such a scheme would predict a decrease of the rate of formation of the transient, when the $Cu(II)EDTA^{2-}$ concentration is raised.

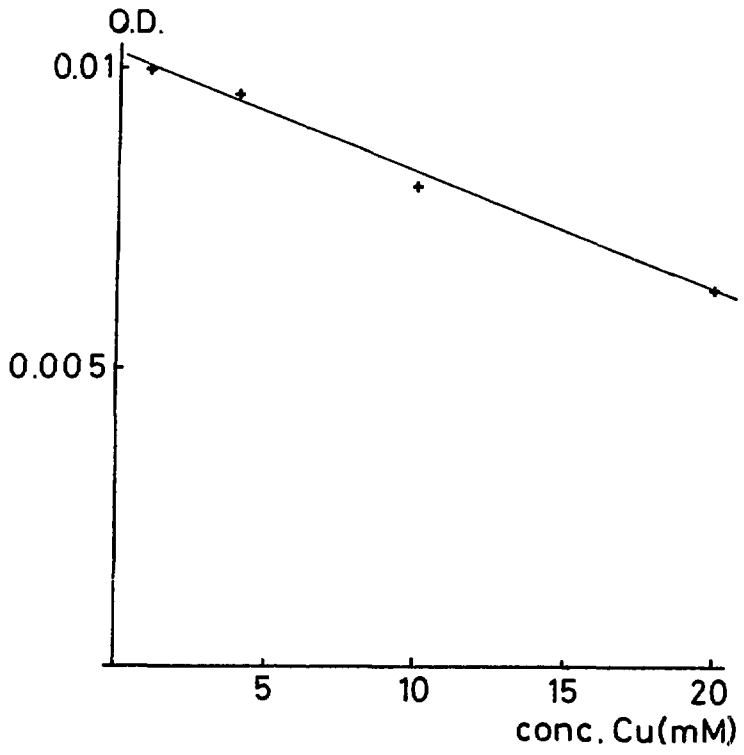

Fig. 5 Influence of the $Cu(II)EDTA^{2-}$ concentration on the final O.D. at 440 nm of copper complexed with EDTA and n-butanol radical. The concentration of n-butanol is 60 mM, pH is 7.5 (phosphate buffer)

The increase of the rate of formation and the decrease of the yield of the transient can be explained adequately by a reaction scheme as represented by the combined reactions 4 and 7. In Figure 6 the generalized behaviour of such a system is shown, as calculated by the WR16 program for different ratios of k_4 and k_7. It shows that the final yield of the transient (the intercept in Figure 6) decreases and the - apparent - rate of formation increases if the concentration of $Cu(II)EDTA^{2-}$ is raised. The apparent rate of formation is proportional to the inverse of $T_{\frac{1}{2},f}$, which is found in

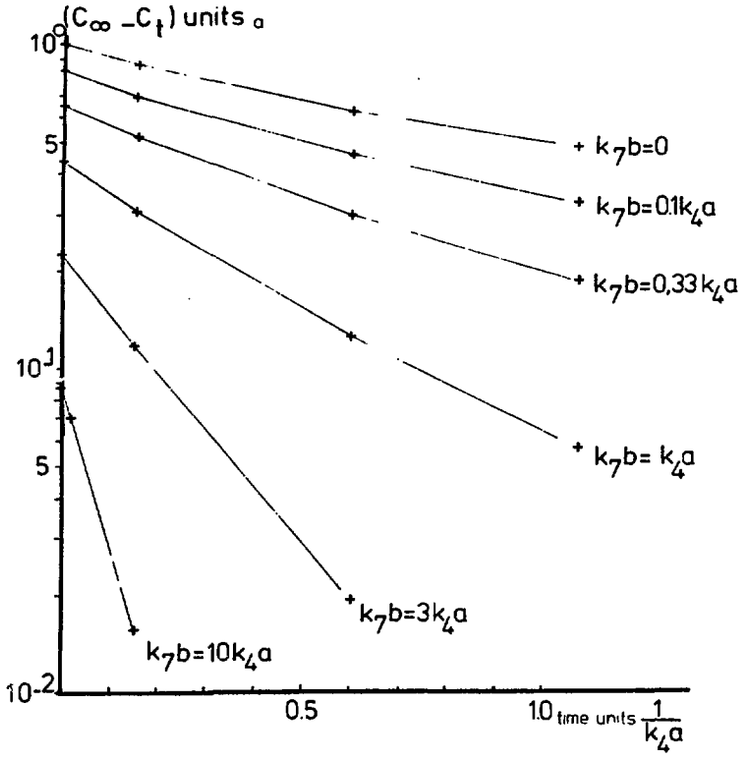

Fig. 6 Kinetic behaviour of a system consisting of two concurrent second-order reactions:
$RHOHC\cdot + Cu(I)EDTA^{3-} \xrightarrow{k_4} RHOHCCu(II)EDTA^{3-}$
$RHOHC\cdot + Cu(II)EDTA^{2-} \xrightarrow{k_7}$ products
Assumed is: $[RHOHC\cdot]_{t=0} = [Cu(I)EDTA^{3-}]_{t=0} = a$; $[RHOHCCu(II)EDTA^{3-}]_{t=0} = 0$; $[Cu(II)EDTA^{2-}]_{t=0} = b$, $b >> a$. c_∞ = maximum concentration of the transient, c_t = concentration at time t.

Figure 6 as the time at which the value of $(c_\infty - c_t)$ is decreased to half the value of the intercept.

In addition the influence of NO_3^- ions on the system was studied. Nitrate is a very efficient scavenger for solvated electrons:

$$NO_3^- + e_{aq}^- \rightarrow NO_3^{2-} \quad k_8 = 1.1 \times 10^{10}\ M^{-1}s^{-1}\ 13) \qquad (8)$$

Reactions 3 and 8 compete for the available e_{aq}^- if nitrate is added to the system with the result that the concentration of $Cu(I)EDTA^{3-}$ is decreased (Figure 7a). On the assumption

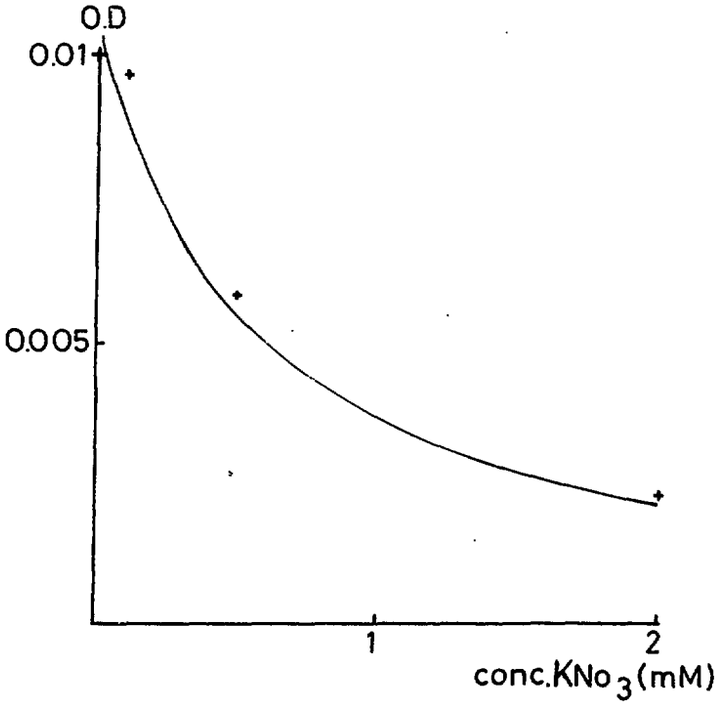

Fig. 7a Influence of NO_3^- on the final yield of $CH_3(CH_2)_2HOHCCu(II)EDTA^{3-}$. $[Cu(II)EDTA^{2-}]$ = 1 mM, [n-butanol] = 60 mM, pH = 7 (phosphate buffer).

that the quantity of the transient species represents an approximately constant fraction of the $Cu(I)EDTA^{3-}$, its yield is given by the following equation:

$$\frac{O.D._{max}}{O.D.} = 1 + R\ \frac{[NO_3^-]}{[Cu(II)EDTA^{2-}]} \qquad (II)$$

The meaning of the symbols used is the same as in equation (I), R is here the ratio of k_8 and k_3. From the value of R, which

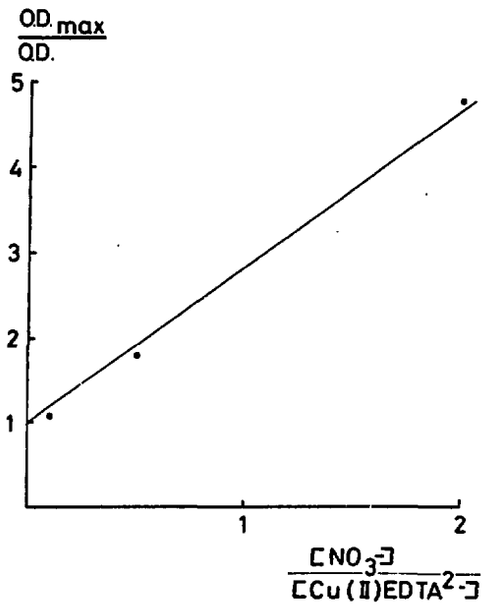

Fig. 7b The data from Figure 7a represented according to equation (II), which describes the effect of the concurrent reactions of the solvated electron with $Cu(II)EDTA^{2-}$ and NO_3^-

can be derived from Figure 7b we calculate for k_3: $6 \times 10^9\ M^{-1}s^{-1}$. This value compares very well with the measured one mentioned in Chapter IV for the reaction of the solvated electron with $Cu(II)EDTA^{2-}$ at a similar ionic strength.

The formation of the transient by reaction 4 is not only complicated by reaction 7, the contribution of which can be kept small by using a low concentration of $Cu(II)EDTA^{2-}$, but also by the - dimerization - reaction of the alcohol radicals [14]:

$$RHOHC\cdot + RHOHC\cdot \rightarrow \text{glycols} \qquad (9)$$

The reaction rate constant k_9 is about $10^9\ M^{-1}s^{-1}$ for n-butanol radicals [14].

To evaluate the influence of this reaction a number of calculations by means of the WR16 program have been performed, assuming a dose of 10 Gy. These calculations showed a net build-up of $Cu(I)EDTA^{3-}$ due to reaction 9, even if $k_4 = 5\ k_9$. This results in a decrease of $T_{\frac{1}{2},f}$ at prolonged irradiations (more pulses), which is in accordance with the experimental observations.

When experiments were done with $Cu(II)EDTA^{2-}$ at different pH in the presence of n-butanol, it appeared that the final yield of $RHOHCCu(II)EDTA^{3-}$ at pH 11.5 was about half the final yield obtained at a lower pH (pH = 8.5 and pH = 7.5). A possible explanation would be that the alpha-radical from n-butanol has an acid-base equilibrium with $pK_a = 11.5$ [16]. This, however, does not explain the reduction of the yield of the transient because the acid-base equilibrium is established very rapidly [16] and thus it cannot be rate-determining. This has been verfied by calculations by means of the WR16 program, taking into account the known rates of dimerization of the alcohol radicals in the acid and the basic state [14]. The variation of the yield with pH is probably due to the fact that at a high pH the Cu(II)EDTA complex is present in a hydrolysed form: $Cu(II)(OH)EDTA^{3-}$ [10,15].

At pH = 11.5 it is possible by the addition of N_2O to obtain yields of the transient comparable with the yield at lower pH. The reason for this is not yet clear. Calculations in which part of the e^-_{aq} is assumed to react with N_2O at the expense of the formation of $Cu(I)EDTA^{3-}$ and in which a delayed formation of extra alcohol radicals by N_2O products was assumed, did not explain the observed effect.

At pH = 7.5 no influence on the yield of the transient was observed with N_2O, but the $T_{\frac{1}{2},f}$ increases by a factor of two to three compared with the samples without N_2O.

5.5 *Estimates of rate constants and extinction coefficients*

The evaluation of rate constant k_4 is difficult. First there are the reactions 7 and 9, which influence disappearance of one of the reactants (RHOHC·) of reaction 4 and cause a net build-up of Cu(I) products. Because of the repetitive character of the measurements this build-up changes the composition of the reaction mixture during the measurements, resulting in a decrease of $T_{\frac{1}{2},f}$ during prolonged irradiations. Consequently, all evaluations of $T_{\frac{1}{2},f}$ will be underestimates.

Under these circumstances it is possible to obtain only an estimate of the upper limit of k_4. This was done in the case of n-butanol and $Cu(II)EDTA^{2-}$. The estimates of k_4 in the case of the other alcohols appear to be of the same order of magnitude.

A typical experiment performed at pH = 7.5 (phosphate buffer) and with a dose of 13 Gy yielded: $T_{\frac{1}{2},f} \simeq 40$ µs, final yield = 0.013 O.D. (440 nm). At this dose the concentrations immediately after the electron pulse are: 4.2 µM alcohol radicals and 3.5 µM $Cu(I)EDTA^{3-}$ according to the reactions 1 to 3. The concentration of $Cu(II)EDTA^{2-}$ was 1 mM and it is known from the experiment shown in Figure 5 that at this concentration reaction 7 was of little consequence. A set of calculations was performed with the aid of the WR16 program concerning the influence of reactions 4 and 9 on the yield, using various values for k_4 and k_9. If the value of k_9 was chosen smaller than or equal to 2×10^9 $M^{-1}s^{-1}$, a value of 40 µs for $T_{\frac{1}{2},f}$ was obtained when $k_4 = 5 \times 10^9$ $M^{-1}s^{-1}$. This is the maximum value of the rate constant because of the net build-up of $Cu(I)EDTA^{3-}$ from pulse to pulse due to reaction 9: e.g. 0.9 µM per pulse for $k_9 = 2 \times 10^9$ $M^{-1}s^{-1}$, 0.4 µM per pulse for $k_9 = 1 \times 10^9$ $M^{-1}s^{-1}$. The build-up will not be quite as large as suggested by these values, because $Cu(I)EDTA^{3-}$ is not a stable species and it will therefore disappear between the pulses.

The maximum final yield of $RHOHCCu(II)EDTA^{3-}$ as

calculated by the program is ∿ 3 μM. The extinction coefficient at 440 nm of this transient (using n-butanol as OH· scavenger) is then 4.3 x 10^3 $M^{-1}cm^{-1}$, which should be considered as a minimum value.

Figure 5 shows the yield of $CH_3(CH_2)_2HOHCCu(II)EDTA^{3-}$ a function of the concentration of $Cu(II)EDTA^{2-}$. At a concentration of ca. 25 mM the final yield is halved. If we take $k_4 \sim 10^9$ $M^{-1}s^{-1}$, then k_7 can be estimated as $\leq 2 \times 10^5$ $M^{-1}s^{-1}$.

5.6 Chemical properties

The disappearance of $RHOHCCu(II)EDTA^{3-}$ shows an initial half-life of 1 to 3 msec or even longer. Consequently the kinetics can not be measured very well with the present apparatus, which is optimized for the time scale between 1 μs and 1 ms. The mechanism proposed by Cohen and Meyerstein for the hydrolysis of the chromium-carbon bonds [9] may well be applicable to the case of the copper-carbon bonds:

$$RHOHCCu(II)EDTA^{3-} + H_2O \rightarrow Cu(II)(OH)EDTA^{3-} + RHOHCH \quad (10)$$

$$RHOHCCu(II)EDTA^{3-} + H_3O^+ \rightarrow Cu(II)EDTA^{2-} + RHOHCH + H_2O \quad (11)$$

Such a conclusion remains to be verified on an apparatus capable of covering the appropriate time scale.

It was notices that the presence of NO_2^- increased the rate of disappearance of $RHOHCCu(II)EDTA^{3-}$:

$$RHOHCCu(II)EDTA^{3-} + NO_2^- \rightarrow \text{products} \quad (13)$$

The second order rate constant k_{12} was 4.0 x 10^5 $M^{-1}s^{-1}$ (RH = n-butanol), measured at two concentrations of NO_2^-.

References

1) D. Meyerstein, Inorg. Chem. 10 (1971) 638

2) D. Meyerstein, Inorg. Chem. 10 (1971) 2244

3) S.N. Bhattacharyya and K.P. Kundu, Int. J. Radiat. Phys. Chem., 5 (1973) 183

4) N. Basco, S.K. Vidyarthi and D.C. Walker, Can. J. Chem. 52 (1974) 343
5) G.E. Adams and R.L. Willson, Trans. Far. Soc. 65 (1969) 2981
6) M. Kelm, J. Lilie and A. Henglein, J. Chem. Soc. 75 (1975) 1132
7) M. Kelm, J. Lilie, A. Henglein and E. Janata, J. Phys. Chem. 78 (1974) 882
8) G.V. Buxton and R.B. Sellers, J. Chem. Soc., Far. Trans I, 71 (1975) 558
9) H. Cohen and D. Meyerstein, Inorg. Chem. 13 (1974) 2434
10) G. Schwarzenbach, Helv. Chim. Acta 32 (1949) 839
11) L.M. Dorfmann and G.E.D. Adams, NSRDS-NBS 46 (1973)
12) M. Anbar, Farhataziz and A.B. Ross, NSRDS-NBS 51 (1975)
13) M. Anbar, M. Bambenek and A.B. Ross, NSRDS-NBS 43 (1973)
14) M. Simic, P. Neta and E. Hayon, J. Phys. Chem. 73 (1969) 3794
15) G. Schwarzenbach and H. Ackermann, Helv. Chim. Acta 30 (1947) 1798
16) K.-D. Asmus, A. Henglein, A. Wigger and G. Beck, Ber. Bunsenges. Phys. Chem. 70 (1966) 756

CHAPTER VI

THE RADIOLYSIS OF $Cd(II)EDTA^{2-}$ AND $Pb(II)EDTA^{2-}$

6.1 *Introduction*

The radiolysis of $Cd(II)EDTA^{2-}$ and $Pb(II)EDTA^{2-}$ can be readily studied because the product of the reaction of these species with the solvated electron shows an optical absorption spectrum:

$$e^-_{aq} + Cd(II)EDTA^{2-} \rightarrow Cd(I)EDTA^{3-} \quad (1)$$

$$e^-_{aq} + Pb(II)EDTA^{2-} \rightarrow Pb(I)EDTA^{3-} \quad (2)$$

This makes it possible to illustrate the reaction scheme described in section 3.1 for other ligands than H_2O. The measurement of k_1 and k_2 is described in Chapter IV.

The spectrum of $Cd(I)EDTA^{3-}$ was investigated earlier by Meyerstein *et al.* [1]. However, accurate determination of the absorption spectrum was complicated by the reactions:

$$OH\cdot + EDTA^{4-} \rightarrow \text{products} \quad (3)$$

$$H\cdot + EDTA^{4-} \rightarrow \text{products} \quad (4)$$

The EDTA to Cd ratio was 2 : 1 in the measurements of Meyerstein *et al.* In our work the reactions (3) and (4) were suppressed by the addition of alcohols and by reducing the excess of EDTA to ten percent

We also established the relative redox potentials for the Cd(I)/Cd(II) and Pb(I)/Pb(II) couples complexed by EDTA by demonstrating the occurrence of reaction (5):

$$Cd(I)EDTA^{3-} + Pb(II)EDTA^{2-} \rightarrow Cd(II)EDTA^{2-} + Pb(I)EDTA^{3-} \quad (5)$$

These couples were investigated by Baxendale *et al.* [2] by the same method in the case of water complexes.

6.2 *Experimental*

The samples used for the determination of the spectra contained 10 to 20 mM $CdSO_4$ or $PbCl_2$, an excess of Na_2H_2EDTA of less than ten percent and 60 mM alcohol. The solutions were adjusted to pH = 11.5 by means of NaOH. The quality of the chemicals and the water was as described in Chapter II. The samples were deaerated by means of the freeze-thawing technique and irradiated with doses between 5 and 10 Gy. Dosimetry was performed with the e^-_{aq} dosimeter at 550 or 600 nm.

The samples used for the investigation of the formation of Cd(I)EDTA and Pb(I)EDTA contained 1 to 2 mM $CdSO_4$ or 0.1 to 0.2 mM $PbCl_2$, EDTA to an excess of less than ten percent and 60 mM n-butanol, adjusted to pH = 11.5.

The composition of the samples used for the measurement of reaction (5) were: 30 mM $CdSO_4$, 1.6 mM $PbCl_2$, 35 mM EDTA and NaOH to a pH of 11.5 or alternatively: 50 mM $CdSO_4$, 3 mM $PbCl_2$, 60 mM EDTA and NaOH to a pH of 11.5. In both cases we also added 60 mM butanol-1.

6.3 *Formation of transient cadmium or lead species by e^-_{aq} reactions*

The reactions (1) and (2) were discussed in Chapter IV. The charge on the Cd(II)EDTA and the Pb(II)EDTA ions, which react according to reactions (1) and (2) is -2. This was demonstrated by performing experiments at different values for the ionic strength. Apparently in this case it is not necessary to account for equilibrium [3,4,5].

$$M(II)EDTA^{2-} + OH^- \rightleftarrows M(II)(OH)EDTA^{3-} \qquad (6)$$

A fair indication for the transformation of one kind of transient into another can be obtained by measuring absorption spectra of the sample at different times after the pulse of ionizing radiation. Reaction (1) was followed in this way, as shown in Figure 1. One can see that the absorption due to e^-_{aq} (λ_{max} = 720 nm) decreases while at the same

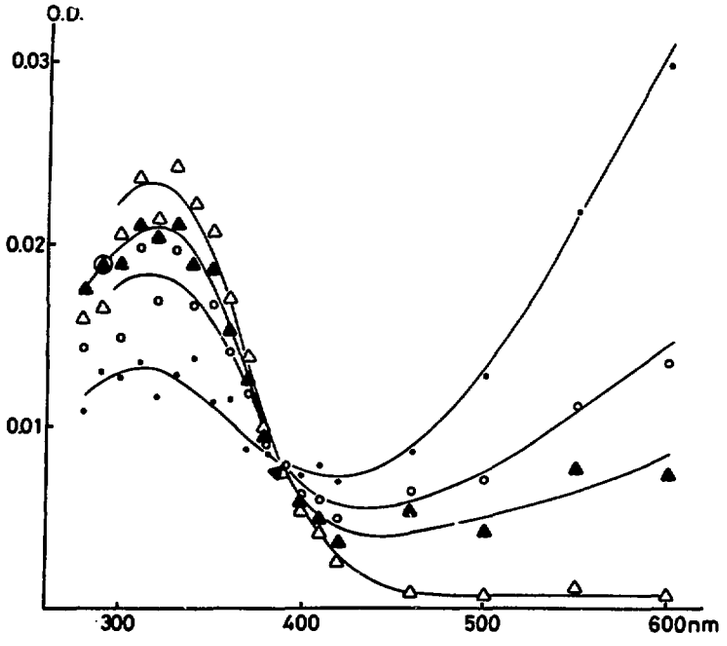

Fig. 1 e^-_{aq} + Cd(II)EDTA^{2-} → Cd(I)EDTA^{3-}
[Cd(II)EDTA^{2-}] = 10^{-3} M. $\lambda_{max}(e^-_{aq})$ = 715 nm,
λ_{max}(Cd(I)EDTA^{3-}) = 320 nm.
. Absorption spectrum 1 μs after the pulse
o Absorption spectrum 3 μs after the pulse
▲ Absorption spectrum 5 μs after the pulse
Δ Absorption spectrum 13 μs after the pulse

time the intense absorption due to Cd(I)EDTA^{3-} (λ_{max} = 320 nm) increases. Consequently an isobestic point is observed at 390 nm in this figure. It is concluded that reaction (1) describes the situation satisfactory.

To avoid complications due to the products of the reactions of H· and OH· radicals with EDTA (reaction (3) and (4)), the excess of EDTA was kept small (ten percent or less) and an alcohol (normally n-butanol) was added to the mixture:

$$RHOHCH + OH\cdot \rightarrow RHOHC\cdot + H_2O \qquad (7)$$

$$RHOHCH + H\cdot \rightarrow RHOHC\cdot + H_2 \qquad (8)$$

The concentration of n-butanol (60 mM) used is sufficient because $k_3 = 2.8 \times 10^9\ M^{-1}s^{-1}$ [6] and k_7 and k_8 are respectively $4.0 \times 10^9\ M^{-1}s^{-1}$ and $3.8 \times 10^7\ M^{-1}s^{-1}$ [7,8]. It is uncertain whether the H· radical is involved in processes other than reaction (8). It might be that the H· radical like e^-_{aq} can reduce the cadmium to the monovalent state. This seems unlikely because $k(H\cdot + Cd^{2+}_{aq})$ is relatively small: $\leq 3 \times 10^5\ M^{-1}s^{-1}$ [8]. Another possibility is that the H· radical - like the OH· radical [6] - degrades the EDTA-ligand. However, these additional reaction pathways cannot be very important, even when these reactions are fast (for comparison: the half-life of the H· radicals is 0.3 μs, based on reaction (8) at our n-butanol concentration). In the case of fast H· reactions the maximum final yields of the products will be too small the be significant in comparison with the yields of the same products generated by the other primary species, as $G_{H\cdot}$ is approximately twenty percent of $G_{OH\cdot}$ or $G_{e^-_{aq}}$.

Another reaction which is also suppressed to a large extent by the addition of the alcohol is

$$OH\cdot + M(II)EDTA^{2-} \rightarrow \text{products} \qquad (9)$$

As already discussed in the previous chapter, dealing with $Cu(II)EDTA^{2-}$ also this rate constant can be quite large. An estimate of k_9 for M = Cd will be given in section 6.6.

6.4 Spectral properties

The transient species $Cd(I)(H_2O)^+_6$ and $Cd(I)EDTA^{3-}$ both absorb strongly around 300 nm as already mentioned in Chapter III. To show that we are dealing with two different species, both transient spectra were measured.

The spectrum of $Cd(I)(H_2O)^+_6$ is shown in Figure 2. The pH was approximately 5 to 6 and t-butanol was used as OH· scavenger. A comparison between the spectral properties we measured and those from other reports is given in Table 1.

The spectrum of $Cd(I)EDTA^{3-}$ is shown in Figure 3 and

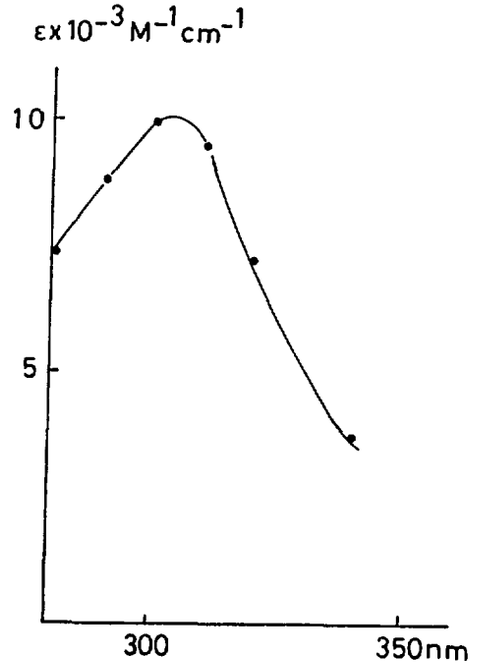

Fig. 2 Absorption spectrum of $Cd(I)^{+}_{aq}$

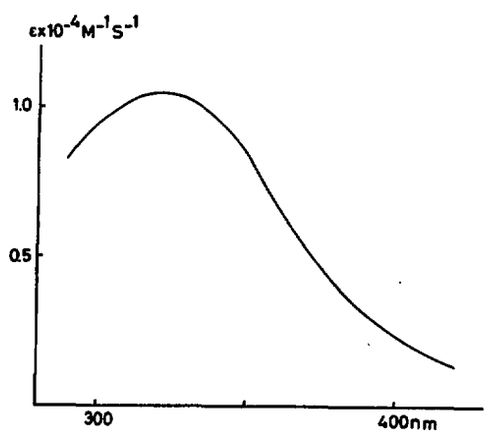

Fig. 3 Absorption spectrum of $Cd(I)EDTA^{3-}$. The curve is the average of many experiments

Table 1 Spectral properties of Cd(I) transient species

Ligand	λ_{max}(nm)	$\varepsilon_{max} \times 10^{-3}$ $M^{-1}cm^{-1}$	Reference
H_2O	304 ± 3	10.0 ± 1.5	this work
	300 ± 5	8.08	9
	300	7.5	10
	300	16	11
EDTA	320 ± 5	10.5 ± 1.5	this work
	∿ 320	2.2 *	1
CDTA	335 ± 10	7.5 ± 1.1	this work

* Recalculated by us from the data of Meyerstein *et al.*, the value listed is at 350 nm, not at λ_{max}.

the spectral properties are quoted in Table 1. The differences from the $Cd(I)(H_2O)_6^+$ spectrum are a slight red shift of the maximum and a much broader absorption peak. At 350 nm the absorption coefficient (ε_{350}) is 8 x 10^3 $M^{-1}cm^{-1}$.

Meyerstein *et al.* have studied a series of Cd-complexes [1]. They found for $Cd(I)EDTA^{3-}$: λ_{max} ∿ 320 nm. The uncertainty in λ_{max} was introduced by absorbing products from the reactions of EDTA with OH· and H· radicals (reactions (3) and (4)). The absorption coefficients at 350 nm (ε_{350}) calculated by them are in the region of 8 x 10^3 $M^{-1}cm^{-1}$ for all Cd(I) complexes (ligands were glycine, ethylene diamine, nitrilotracetic acid and EDTA). However, on the basis of their own method of calculation, we recalculated in the case of $Cd(I)EDTA^{3-}$ a much lower value: ε_{350} = 2.2 x 10^3 $M^{-1}cm^{-1}$. This value was calculated by subtracting the optical density obtained in a pure EDTA solution from the optical density in a $Cd(II)EDTA^{2-}$ and EDTA mixture, to account for the reactions (3) and (4). The difference from the value for ε_{350} we measured can perhaps be explained by the fact that reaction (9) was ignored in the calculation of Meyerstein *et al.* If the product of this reaction does not have an intense absorption

spectrum in the wavelength interval studied, then the correction on the optical density due to the EDTA products (reactions (3) and (4)) will be too large in the case of Meyerstein *et al.*. The product of reaction (9) is probably Cd(II) complexed with a degraded EDTA molecule, which would have an absorption spectrum similar to that of Cd(II)EDTA, which does not absorb strongly in this region.

The influence of the ligand on the absorption spectrum was investigated by replacing EDTA by CDTA (cyclohexylene-tetra-acetic acid). The position of the maximum is shifted towards the red and the absorption peak is broader than it is for $Cd(I)EDTA^{3-}$ (Figure 4, Table 1).

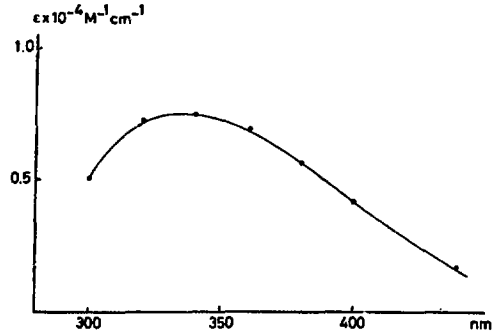

Fig. 4 Absorption spectrum of $Cd(I)CDTA^{3-}$

Reaction (2) (e^-_{aq} with $Pb(II)EDTA^{2-}$) is very similar to reaction (1) (e^-_{aq} with $Cd(II)EDTA^{2-}$). The absorption spectrum of the product of reaction (2) ($Pb(I)EDTA^{3-}$) is shown in Figure 5. The maximum lies below 290 nm, which is beyond the limits of sensitivity of our detection system (Chapter II). The extinction coefficient of $Pb(I)EDTA^{3-}$ is smaller than the extinction coefficient of $Cd(I)EDTA^{3-}$ in the wavelength interval studied. Baxendale *et al.* [10] made a similar observation for $Pb(I)(H_2O)^{+}_{6}$ and $Cd(I)(H_2O)^{+}_{6}$.

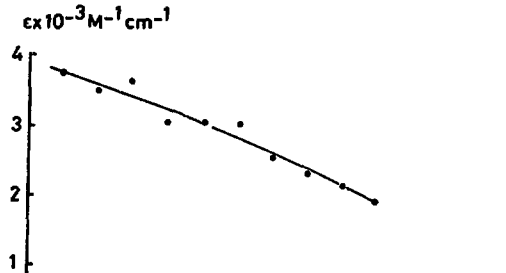

Fig. 5 Absorption spectrum of $Pb(I)EDTA^{3-}$

6.5 The influence of H_2O_2

During the irradiation H_2O_2 is formed with an initial G-value of 0.68 [12]. This formation can be partially suppressed by means of a large amount of OH· scavenger, according to the spur theory [13,14]. For example, reducing of the initial G-value to 0.51 requires approximately 100 mM ethanol. The rate constant k_7 is 1.8×10^9 $M^{-1}s^{-1}$ in the case of ethanol [7]. It is clear that this is not an efficient process. In practice for each case one has to evaluate the influence of the H_2O_2 formed during the irradiation.

In the literature the reaction of H_2O_2 with monovalent aqueous ions is described [15,16]:

$$H_2O_2 + M(H_2O)_6^+ \rightarrow M(H_2O)_6^{2+} + OH\cdot + OH^- \qquad (10)$$

For $Cd(I)(H_2O)_6^+$ the rate constant k_{10} is 2×10^9 $M^{-1}s^{-1}$. It is reasonable to expect that reaction (11) also has a large rate constant:

$$H_2O_2 + Cd(I)EDTA^{3-} \rightarrow Cd(II)EDTA^{2-} + OH\cdot + OH^- \qquad (11)$$

If this is the case it should be visible in the decay of the transient absorption of $Cd(I)EDTA^{3-}$. Experimentally it is shown that the decay curve consists of at least two components, one of which acts only for about a μs. This decay was measured for

a series of alcohols, but for reasons to be discussed in the next paragraph, only the decay in the presence of 60 - 70 mM t-butanol was considered.

In Figure 6 both the experimental and calculated decays are shown. For the calculated lines the WR16 program

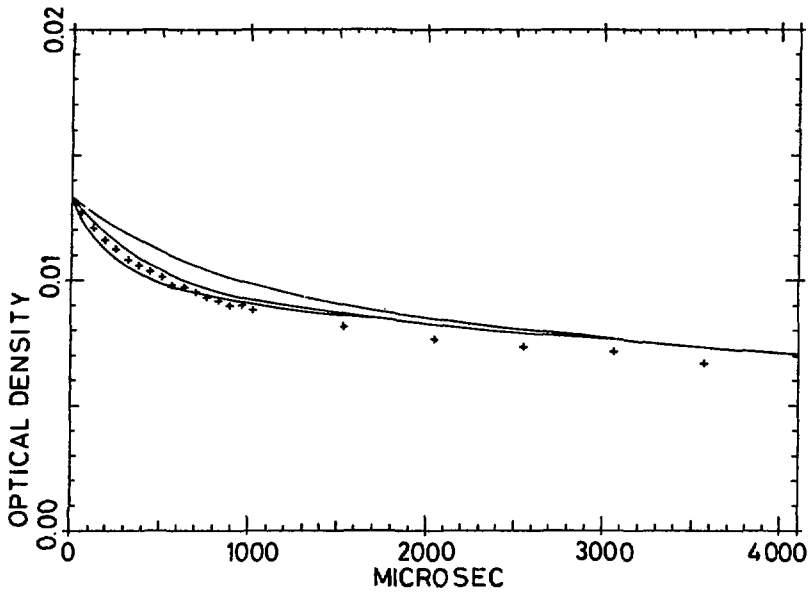

Fig. 6 Experimental (+) and calculated decay of $Cd(I)EDTA^{3-}$ (solid lines) in the presence of t-butanol (67 mM) due to the reaction with H_2O_2. The calculated lines represent from top to bottom: $k_{11} = 1.0 \times 10^9\ M^{-1}s^{-1}$, $k_{11} = 2.0 \times 10^9\ M^{-1}s^{-1}$ and $k_{11} = 3.0 \times 10^9\ M^{-1}s^{-1}$. The initial yields assumed were: $G(Cd(I)EDTA^{3-}) = G_{e^-_{aq}} = 2.7$, $G_{H_2O_2} = 0.7$.

used reaction (11), a first order rate constant of 80 s^{-1} for the second component of the decay and the following initial yields:

i) $G(Cd(I)EDTA^{3-}) = G_{e^-_{aq}} = 2.7$

ii) $G_{H_2O_2} = 0.7$.

When k_{11} is taken equal to $2 \times 10^9\ M^{-1}s^{-1}$, a fair description of the kinetic behaviour is obtained, at least in the first

0.5 ms.

To confirm this result an additional experiment was done in which H_2O_2 was added in a concentration of 130 μM. We were compelled to use such a small amount of H_2O_2 because of the limitations of the detection system. Although we tried to correct for the repetitive character of our measurements, we obtained only a lower limit for k_{11}: $\geq 2 \times 10^8$ $M^{-1}s^{-1}$.

The decay of $Pb(I)EDTA^{3-}$ is similar to the decay of $Cd(I)EDTA^{3-}$.

$$H_2O_2 + Pb(I)EDTA^{3-} \rightarrow Pb(II)EDTA + OH\cdot + OH^- \qquad (12)$$

The value for k_{12} obtained, using the WR16 program was 2.5×10^9 $M^{-1}s^{-1}$. In this case the error was large (∿50%) due to the small absorption coefficient.

6.6 The influence of alcohols on the decay of $Cd(I)EDTA^{3-}$

The decay of the $Cd(I)EDTA^{3-}$ absorption is influenced by several factors, one of which (reaction (11)) was already discussed in the previous section. According to the general scheme proposed in section 3.1, one has to consider the reaction of the radicals formed by the reactions (7) and (8), with $Cd(I)EDTA^{3-}$:

$$RHOHC\cdot + Cd(I)EDTA^{3-} \begin{cases} \rightarrow RHOHC\ Cd(II)EDTA^{3-} & (13a) \\ \rightarrow \text{other products} & (13b) \end{cases}$$

For the product of reaction (13a) one can think of a pentadentate Cd-EDTA complex where the H_2O on the sixth site is replaced by a carbon-Cd-bond [4,5].

Reaction (13) must be concurrent with reaction (14):

$$2\ RHOHC\cdot \begin{cases} \rightarrow \text{glycols} & (14a) \\ \rightarrow \text{alcohol + aldehyde (ketone)} & (14b) \end{cases}$$

The values of k_{14} together with other relevant information are given in Table I of Chapter III (k_{14} is listed as 'k_8' in this table). Reaction (13) competes with reaction (14) only if the rate constants are of the same order of magnitude: ∿ 10^9 $M^{-1}s^{-1}$.

If one takes a series of alcohols, one can estimate the importance of reaction (13) either by measuring the decay of Cd(I)EDTA at a time when the H_2O_2 formed during the pulse is largely consumed (reaction (11)), or by comparing the optical density 65 µs after the pulse and the optical density some 4 ms later.

The first method has been used to obtain Figure 7, where the average decay constant (first order) between 3 and 6 ms is plotted as a function of the percentage of alpha-radicals yielded by reactions (7) and (8) (Table I of Chapter III).

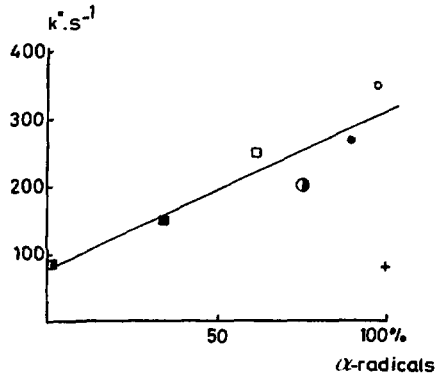

Fig. 7 Influence of alcohols on the decay of $Cd(I)EDTA^{3-}$. k^x = average (pseudo-) first order decay constant between 3 ms and 6 ms.
+: methanol, o: ethanol, □:propanol-1,
•: propanol-2, ■: butanol-1, ◑: butanol-2,
◘: t-butanol

All points are scattered around a straight line with the exception of the point representing the methanol radical.

The second method is shown in Figure 8, once more as a function of the percentage of alpha-radicals. Both methods

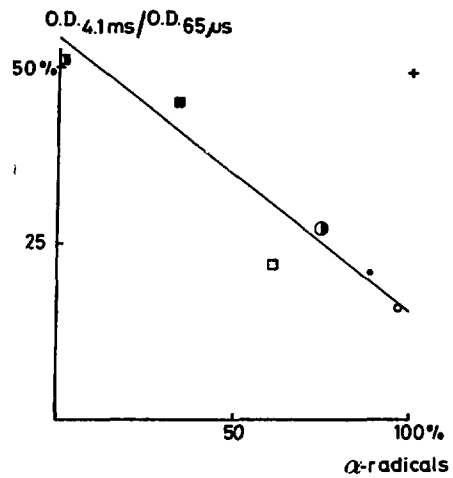

Fig. 8 Influence of alcohols on the decay of $Cd(I)EDTA^{3-}$
+: methanol, o: ethanol, □: propanol-1,
•: propanol-2, ■: butanol-1, ◑: butanol-2,
◘: t-butanol

suggest a correlation between the percentage of alpha-radicals yielded by reactions (7) and (8) and the rate of reaction (13), with the exception of the methanol radical. In Table 2 of Chapter III one can see that for Cd^{+}_{aq} reacting with alcohol radicals also the reaction rate with methanol radicals is one order of magnitude smaller than that with the other alcohol radicals. The choice of t-butanol for the experiment used for the calculation of k_{11} in the previous section is justified, because of the low reactivity according to reaction (13), as is demonstrated in Figures 7 and 8.

For the radicals of ethanol, propanol-2 and butanol-2 there is an indication for the formation of a product (probably resulting from reaction (13a)) absorbing at wavelengths below 300 nm. However, it is also possible that these are products of the reactions (3) and (4),if these reactions were not totally suppressed. This has to be investigated with an apparatus with a detector sensitive at wavelengths below 300 nm and optimized for the ms timescale.

An attempt was made to use the WR16 program to estimate k_{13} for ethanol radicals (97% alpha-radicals), taking

into account the reactions (7), (11) and (14) and a background decay of 80 s^{-1}, as suggested by Figure 7, which originates from hydrolysis, disproportionation or dimerization. It was not possible to fit a calculated decay of $Cd(I)EDTA^{3-}$ with the experimental points in a really satisfactory way. The best estimate for k_{13} (ethanol radicals) is 8×10^8 $M^{-1}s^{-1}$ ± 50%. The rate constant k_{13} for the other alcohol radicals can be estimated from this value and from Figure 7, except for the other decay modes mentioned above (taken into account by assuming a background decay constant of 80 s^{-1}).

The number of alcohol radicals present depends on the concentration of the alcohol because of the competition between reactions (7) and (9). According to equation (13) the average decay constant (first order) between 3 and 6 ms, as used in Figure 7, is a function of the concentration of the alcohol radicals. It is obvious that at high alcohol concentrations all OH· radicals react through reaction (7), which leads to a maximum value of the mean decay constant. At an alcohol concentration which corresponds to a decay constant of half the plateau-value the OH· radicals react equally fast in both channels: $k_7[\text{alcohol}] = k_9[Cd(II)EDTA^{2-}]$. For isopropanol we found this situation at a concentration of about 10 mM. The concentration of $Cd(II)EDTA^{2-}$ was also 10 mM. This means that $k_9 \approx k_7 = 2 \times 10^9$ $M^{-1}s^{-1}$ 7).

6.7 Redox-properties of the transient

$Cd(I)EDTA^{3-}$ has a higher reducing potential than $Pb(I)EDTA^{3-}$, because reaction (5) takes place. This can be studied by taking a large excess $Cd(II)EDTA^{2-}$ in order to favour reaction (1) over reaction (2). To evaluate the rate constant k_5 the optical density at 340 and 360 nm was calculated as a function of time with the aid of the WR16 program, taking into account k_1, k_2, k_{11}, k_{12} and the extinction coefficients of $Cd(I)EDTA^{3-}$ and $Pb(I)EDTA^{3-}$ and the results were compared with the measured values. In this calculation it was

necessary to postulate reaction (15):

$$Cd(I)EDTA^{3-} + Pb(II)EDTA^{2-} \rightarrow \text{product X} \qquad (15)$$

The reason is that the optical density was about a factor two lower than if only $Pb(I)EDTA^{3-}$ had been formed. The absorption spectrum measured at three wavelengths after the completion of reactions (5) and (15) was similar to the spectrum of $Pb(I)EDTA^{3-}$. We postulate therefore that product X absorbs even less than $Pb(I)EDTA^{3-}$ does. Under these assumptions $k_5 + k_{15}$ is equal to about 4×10^6 $M^{-1}s^{-1}$ (total ionic strength $\mu = 0.25$). This value was obtained for two concentrations of $Pb(II)EDTA^{2-}$.

The product of the charges on the reactants of reaction (5) and (15) can be evaluated with the Debye-Hückel theory as explained in Chapter IV. Because of the uncertainties in the reaction radius and the measurements themselves and also because of the high concentrations in the mixtures, the only conclusion that can be drawn is:
$Z(Cd(I)EDTA) \times Z(Pb(II)EDTA) \geq +2$. This confirms that our assumption that the reactions (5) and (15) are reactions between negatively charged species is correct.

References

1) D. Meyerstein and W.A. Mulac, Inorg. Chem. 9 (1970) 1762
2) J.H. Baxendale, J.P. Keene and D.A. Stott, Chem. Comm. 20 (1966) 715
3) M. Anbar and D. Meyerstein, Trans. Far. Soc. 65 (1969) 1812
4) G. Schwarzenbach and H. Ackermann, Helv. Chim. Acta 30 (1947) 1798
5) G. Schwarzenbach, Helv. Chim. Acta 32 (1949) 839
6) S.N. Bhattacharyya and K.P. Kundu, Int. J. Radiat. Phys. Chem. 4 (1972) 31
7) L.M. Dorfmann and G.E. Adams, NSRDS-NBS 46 (1973)
8) M. Anbar, Farhataziz and A.B. Ross, NSRDS-NBS 51 (1975)

9) G.V. Buxton and R.M. Sellers, J. Chem. Soc., Far. Trans. I, 71 (1975) 558

10) J.H. Baxendale, E.M. Fielden and J.P. Keene, Proc. Roy. Soc., Ser. A 286 (1965) 320

11) M. Kelm, J. Lilie and A. Henglein, J. Chem. Soc. 75 (1975) 1132

12) E.J. Hart, Rad. Res. Rev. 3 (1972) 285

13) J.D. Backhurst, R.A. Johnson, G. Scholes and J. Weiss, Nature 183 (1959) 176

14) J.K. Thomas in: Advances in Radiation Chemistry, Vol. 1, Ed. M. Burton and J.L. Magee, J. Wiley and Sons, Inc. (1969) 119

15) D. Meyerstein and W.A. Mulac, J. Phys. Chem. 72 (1968) 784

16) G.V. Buxton, R.B. Sellers and D.R. McCracken, J. Chem. Soc., Far. Trans. I, 72 (1976) 1464

SUMMARY

The work described in this thesis consists of two parts: first the construction of a computerized pulse radiolysis system with available means, appropriate for the wavelength interval between 300 and 1000 nm, and second the investigation of the radiolysis of aqueous solutions of EDTA complexes in the presence of alcohols.

In Chapter I the background of the subjects and methods is described.

Chapter II describes the measuring system, the registration of the signal, the necessary computer programs, and also the limitations of the system. Hereafter the preparation of the samples to be irradiated is described. Then the performance achieved with this system is demonstrated by the measurement of two well-known entities: e^-_{aq} and $(CNS)^-_2$. At the end of this chapter the dosimetry is discussed.

A general radiolytic reaction scheme of metal complexes in the presence of different alcohols is discussed in Chapter III. Extrapolating from the available literature about hydrated metal ions, it is proposed here that also in the case of EDTA complexes reduced by the hydrated electron, the formation of a mixed complex with the alcohol radicals generated by $OH^\cdot$ and $H^\cdot$ plays an important role.

Chapter IV deals with the reaction of the hydrated electron with EDTA and the EDTA complexes of Cu, Hg, Co, In, Ni, Ga, Mn, Zn, Pb and Cd. The reaction rate constant of the hydrated electron with EDTA is a function of pH. The reaction rate constants of the hydrated electron with this series of EDTA complexes were measured as a function of the ionic strength. The absorption spectra of the products

of these reactions are described.

In Chapter V the properties of mixed complexes formed by $Cu(I)EDTA^{3-}$ and alcohol radicals are described. An estimate is given of the reaction rate constants involved and the extinction coefficient of the mixed complex in the case of n-butanol. In addition the influence on the reaction scheme of the various concurrent reactions is described.

The absorption spectra of the reactions of hydrated electrons with $CdEDTA^{2-}$ or $PbEDTA^{2-}$ are described in more detail in Chapter VI. In the case of cadmium the spectrum is compared with the spectra of $Cd(I)CDTA^{3-}$ and $Cd(I)(H_2O)_6^+$. The influence of H_2O_2 and alcohol radicals generated during irradiation on the decay of the reduced complexes is discussed and estimates of the reaction rate constants in the case of H_2O_2 are evaluated. In a comparison of the redox properties of $Cd(I)EDTA^{3-}$ and $Pb(I)EDTA^{3-}$ by measuring the reaction rate constant of the reaction between $Cd(I)EDTA^{3-}$ and $Pb(II)EDTA^{2-}$, the former turned out to be the strongest reductor.

SAMENVATTING

Het werk beschreven in dit proefschrift bestaat uit twee gedeelten. Het eerste gedeelte omvat de bouw van een pulsradiolyse systeem gebaseerd op een mini-computer en andere beschikbare apparatuur en geschikt voor het golflengte interval tussen 300 en 1000 nm. Het tweede gedeelte omvat het onderzoek van de radiolyse van EDTA complexen in waterige oplossingen in de aanwezigheid van alcoholen.

In Hoofdstuk I worden de achtergronden van de gebruikte begrippen en methodes beschreven.

Hoofdstuk II beschrijft de meetopstelling, de registratie van de gegevens, de benodigde computerprogramma's en de beperkingen van het meetsysteem. Hierna wordt de bereiding van de te bestralen preparaten beschreven. Vervolgens wordt de kwaliteit van het meetsysteem gedemonstreerd aan de hand van twee bekende chemische systemen: e^-_{aq} en $(CNS)^-_2$. Tenslotte wordt de dosimetrie bediscussieerd.

Het algemene radiolyseschema van metaalcomplexen in de aanwezigheid van verschillende alcoholen wordt besproken in Hoofdstuk III. Uitgaande van de beschikbare literatuur over gehydrateerde metaalionen wordt hier gepostuleerd dat ook in het geval van EDTA-complexen, die gereduceerd zijn door het gehydrateerde electron, de vorming van een mengcomplex met de door $OH\cdot$ en $H\cdot$ gevormde alcoholradicalen een belangrijke rol speelt.

Hoofdstuk IV behandelt de reactie van het gehydrateerde electron met EDTA en de EDTA-complexen van Cu, Hg, Co, In, Ni, Ga, Mn, Zn, Pb en Cd. De reactiesnelheidsconstante van het gehydrateerde electron met EDTA blijkt afhankelijk te zijn van de pH. De reactiesnelheidsconstanten van het gehydrateerde electron met de bovenvermelde reeks EDTA-

complexen werden gemeten als functie van de ionsterkte. Verder worden de absorptie spectra van de producten van deze reacties beschreven.

In Hoofdstuk V worden de eigenschappen van mengcomplexen gevormd door $Cu(I)EDTA^{3-}$ en alcoholradicalen beschreven. Een schatting wordt gegeven van de betrokken reactiesnelheidsconstanten en de extinctie coëfficient van het mengcomplex in het geval van n-butanol. Verder wordt de invloed op het reactieschema van de diverse nevenreacties besproken.

In Hoofdstuk VI worden de absorptiespectra van de producten van de reacties van gehydrateerde electronen met $CdEDTA^{2-}$ of $PbEDTA^{2-}$ meer in detail beschreven. In het geval van cadmium wordt het spectrum vergeleken met de spectra van $Cd(I)CDTA^{3-}$ en $Cd(I)(H_2O)_6^+$. De invloed van H_2O_2 en alcoholradicalen, gegenereerd tijdens de bestraling, op het verval van de gereduceerde complexen wordt besproken, tesamen met schattingen van de reactiesnelheidsconstanten in het geval van H_2O_2. Bij een vergelijking van de redoxeigenschappen van $Cd(I)EDTA^{3-}$ en $Pb(I)EDTA^{3-}$ door middel van het meten van de reactiesnelheidsconstante van de reactie tussen $Cd(I)EDTA^{3-}$ en $Pb(II)EDTA^{2-}$, bleek de eerstgenoemde de sterkste reductor.

DANKWOORD

Bij het verschijnen van dit proefschrift wil ik graag een ieder die aan de totstandkoming ervan heeft meegewerkt, hartelijk bedanken.

Hooggeleerde Aten, ik acht het mij een voorrecht mijn wetenschappelijke scholing onder Uw leiding te hebben ontvangen. Uw vermogen om orde te scheppen in de chaos door mij aangesleept tijdens onze discussies is van onschatbare waarde geweest.

Zeergeleerde Lindner, dankzij Uw bemoeienissen kon het pulsradiolyse onderzoek van start gaan. Uw kritiek na het doorlezen van het manuscript heb ik met genoegen verwerkt in de definitieve versie.

Zeergeleerde Louwrier, beste Piet, dankzij jouw initiatief is de bouw van het pulsradiolyse systeem mogelijk geworden. De vrijheid die ik had onder jouw leiding, heb ik altijd hogelijk gewaardeerd. Jouw steun op de juiste ogenblikken heeft veel bijgedragen tot het onderzoek en mijn wetenschappelijke vorming.

Mijn dank gaat verder uit naar de heren F.R. Stock en C.N.M. Bakker voor het op virtuoze wijze samenstellen van de grote hoeveelheid preparaten volgens mijn extreme specificaties en naar mejuffrouw H. Kooiman voor het verrichten van enige experimenten bij de ^{60}Co-bron.

Van de afdeling Electronica wil ik de heren E. Bracke en K. Oostveen bedanken voor het oorspronkelijk ontwerp en bouw van het electronische gedeelte. De heer A.H. Kruijer dank ik voor het verrichten van een algehele revisie van dit gedeelte en de hulp tijdens de experimenten als ondanks alle goede zorg er toch nog iets mis ging. In dit verband dank ik verder de heer J. Wisse voor de rol van "interface" met

met de electronische afdeling en zijn hulp bij nacht en ontij.

De medewerkers van de tekenkamer, en wel in het bijzonder de heren J.H.M. Bijleveld en P. Lassing, en van de mechanische werkplaats ben ik erkentelijk voor het ontwerp en de constructie van het mechanische gedeelte.

De heer W. van der Veen wil ik bedanken voor de accurate wijze waarop hij ervoor gezorgd heeft dat ik steeds tijdig voorzien was van de nodige cuvetten en de constructie van gedeelten van onze destillatie-apparatuur.

De medewerkers van de EVA-groep bedank ik voor de zorg die zij hebben besteed aan de uitvoering van mijn bestralingen.

Dat dit proefschrift nu in een leesbare vorm en met een keurig verzorgde lay-out voor U ligt, heb ik te danken aan mevrouw M. Oskam - Tamboezer. Het drukken werd verzorgd door de heer H.J. Hultzer op de hem kenmerkende manier: vlug en netjes.